Ion Transport in the Gramicidin Channel: Molecular Dynamics Study of Single and Double Occupancy

Benoît Roux,*‡ Blaise Prod'hom,‡§ and Martin Karplus‡

*Groupe de Recherche en Transport Membranaire (GRTM), Département de physique, Université de Montréal, Montréal, Canada H3C 3J7 ‡ Department of Chemistry, Harvard University, Cambridge, Massachussets 02138 USA; and § Institut de Physiologie, Faculte de medecine, Université de Lausanne, Lausanne, Switzerland

ABSTRACT The structural and thermodynamic factors responsible for the singly and doubly occupied saturation states of the gramicidin channel are investigated with molecular dynamics simulations and free energy perturbation methods. The relative free energy of binding of all of the five common cations Li^+, Na^+, K^+, Rb^+, and Cs^+ is calculated in the singly and doubly occupied channel and in bulk water. The atomic system, which includes the gramicidin channel, a model membrane made of neutral Lennard-Jones particles and 190 explicit water molecules to form the bulk region, is similar to the one used in previous work to calculate the free energy profile of a Na^+ ion along the axis of the channel. In all of the calculations, the ions are positioned in the main binding sites located near the entrances of the channel. The calculations reveal that the doubly occupied state is relatively more favorable for the larger ions. Thermodynamic decomposition is used to show that the origin of the trend observed in the calculations is due to the loss of favorable interactions between the ion and the single file water molecules inside the channel. Small ions are better solvated by the internal water molecules in the singly occupied state than in the doubly occupied state; bigger ions are solvated almost as well in both occupation states. Water-channel interactions play a role in the channel response. The observed trends are related to general thermodynamical properties of electrolyte solutions.

INTRODUCTION

An important aspect of ion transport in biological channels concerns the nature of ion-ion interactions in the confined environment of a narrow pore. The fact that biological channels may contain more than one permeant ion at a given time was first realized by Hodgkin and Keynes (Hodgkin and Keynes, 1955). They reported unidirectional ion-flux measurements showing that the effective charge-carrying particle in the electrically polarized axon of the cuttlefish *Sepia officinalis*, a potassium-selective channel, was a multimer of a single ion. Since these early studies, manifestations of multiple occupancy have been found in several biological ion channels, including K, Na, and Ca channels. Although the selectivity of the Na channel was explained by rejection of bigger ions, such a model could not describe the high selectivity of the Ca or K channel for calcium or potassium, respectively. In particular, the behavior of K channels is generally understood in terms of multi-ion single file pores (Hille and Schwarz, 1978; Hille, 1984); the Ca-activated K channel may hold four potassium ions simultaneously and the delayed rectifier K channel at least three (Hille, 1984). The existence of multiply occupied states has led to the idea that multiple ion occupancy plays an important functional role in the permeability and selectivity of ion channels. Detailed analysis of the energetics of ion association with the specific binding sites inside Ca-activated K channels indicates that the influence of ion-ion interactions in the multiply occupied single file pore are an essential component of the mechanisms by which these channels succeed in achieving high selectivity while maintaining a large ionic conductance (Neyton and Miller, 1988a; Neyton and Miller, 1988b); ion-ion repulsion appears to be necessary to counterbalance the effect of deep free energy wells. An even more dramatic example of a very selective ion channel with a high throughput is the calcium channel. At submicromolar concentration, calcium is a powerful blocker of the monovalent cation flux through the Ca channel. At high concentration, calcium ion is the only permeant ion through the Ca channel with an apparent binding affinity reduced by 10,000-fold. Here, a model of double occupancy with electrostatic ion-ion repulsion can explain this phenomenon (Hess and Tsien, 1984). An understanding of the microscopic factors responsible for the multiple ion occupancy of membrane channels is thus of interest to physiologists as well as to biophysicists.

In a channel functioning as a multiple ion pore, the movement of the permeant ions is violating the independence rule and is thus highly correlated. From a microscopic point of view, such a mechanism requires a narrow permeation pathway imposing a single file structure and a significant probability of multiply occupied states (Hille and Schwarz, 1978). The channel formed by the pentadecapeptide gramicidin molecule, one of the best characterized molecular pores (Finkelstein and Andersen, 1981), is a useful model system for studying the principles governing ion-ion interactions in the confined environment of a narrow pore. The gramicidin A is particularly well suited for structure-function studies in view of its structural and functional simplicity. The conformation of the ion-conducting channel in the lipid membrane is a N-terminus-to-N-terminus right-handed dimer formed by two single stranded β-helices that is 26 Å long and has a 4-Å diameter (Arseniev et al., 1985; Cornell et al., 1988; Ketchem

Received for publication 14 July 1994 and in final form 29 November 1994.

Address reprint requests to Dr. Benoît Roux, Département de physique, Université de Montréal, C. P. 6128, succ. A, Montréal, Canada H3C 3J7. Tel.: 514-343-7105; Fax: 514-343-7586; E-mail: rouxb@ere.umontreal.ca.

0006-3495/95/03/876/17 $2.00

et al., 1993; Smith et al., 1989); the narrowness of the pore is such that ions and water cannot pass each other, and permeation must proceed through a single file translocation mechanism between the two binding sites during which the ion is interacting predominantly with the backbone carbonyls of the channel (Finkelstein and Andersen, 1981; Roux and Karplus, 1993). Moreover, although the gramicidin channel is only moderately selective for the various monovalent cations, ion fluxes have been shown to exhibit saturation behavior that is indicative of multiple occupancy states similar to those observed with more complex macromolecular structures (Hladky and Haydon, 1972; Hladky and Haydon, 1984). Several lines of evidence demonstrate that gramicidin can be occupied simultaneously by two ions: model-dependent analysis of ion fluxes based on Eyring rate theory suggest that double ion occupancy exists for potassium and cesium (Sandblom et al., 1983); tracer-flux (Schagina et al., 1978; Schagina et al., 1983) and bi-ionic and reversal potential measurements (Urban et al., 1980) show that at least two K^+, Rb^+, or Cs^+ cations can occupy the channel simultaneously. Experimental evidence in support of double occupancy is not as definitive in the case of Na^+ (Procopio and Andersen, 1979); there is no evidence in the case of Li^+. Interpretation of these experimental observations has led to the view that although double occupancy of the gramicidin channel is less favorable than single occupancy for all cations, it is relatively more favorable for the large K^+, Rb^+, and Cs^+ cations than for the small Li^+ and Na^+ cations (O. S. Andersen, personal communication).

Simple considerations cannot account for the observed trend regarding double occupancy. A cation binding site is located near the entrance at each end of the dimer channel (Koeppe et al., 1979; Olah et al., 1991; Smith et al., 1990; Urry et al., 1982a; Urry et al., 1982b; the ion-ion distance in the doubly occupied channel is estimated to be on the order of 20 Å (Olah et al., 1991). At most, one of the binding sites is occupied at low concentration of permeant ion; the two sites may be occupied simultaneously at higher concentration (O. S. Andersen, personal communication). Descriptions based on continuum electrostatic approximations, which are generally valid at large separations in bulk water (Pettitt and Rossky, 1986), have not provided an explanation of the microscopic basis of the ion size dependence of the gramicidin double occupancy (Levitt, 1987). Arguments based on the finite volume available in the interior of the pore also fail because it is the larger cations, presumably occupying more space, that have a higher relative double occupancy.

The goal of this paper, which represents the continuation of an investigation of ion transport with detailed microscopic models based on realistic interactions (Roux and Karplus, 1991a; Roux and Karplus, 1991b; Roux and Karplus, 1993; Roux and Karplus, 1994; Roux and Karplus, 1995), is to examine the microscopic factors responsible for single and double ion occupancy in the gramicidin channel. In the present study, free energy perturbation techniques are used to calculate the relative free energy of all of the five common cations Li^+, Na^+, K^+, Rb^+, and Cs^+ in the singly and doubly occupied channel, as well as in bulk water. An atomic model of the dimer channel is used that is similar to the one used previously to calculate the free energy profile of a single Na^+ ion along the axis of the channel (Roux and Karplus, 1993). The result of that calculation concerning the location of the dominant binding sites and the detailed ligand structure surrounding the Na^+ are supported by the available experimental data. A deep minimum along the calculated free energy profile was located at each extremity of the channel, corresponding to a cation binding site; the calculated binding site is located at 9.3 Å from the center of the channel where the Na^+ is in close contact with the carbonyl of D-Leu^{10}. Experimentally, a pair of symmetrically located ion binding sites are found at 9.6 ± 0.3 Å for Tl^+ based on difference electron density profile from x-ray diffraction on uniformly aligned multilayer membrane samples (Olah et al., 1991). Also, it is observed with ^{13}C solid state NMR with site-specific labeled gramicidin that the chemical shift anisotropy of carbonyl of D-Leu^{10} exhibits a large change in the presence of Na^+ bound to the channel (Smith et al., 1990). The good agreement concerning the position of the binding site suggests that the present atomic model can be used to investigate the structural and thermodynamic factors controlling the single and double occupancy of the channel.

Details about the microscopic model, the empirical energy function, and the computational approach are given and the free energy perturbation technique and the simulation procedure are described. Special care was given to the parametrization of the ion-peptide potential function, which was developed from ab initio calculations (Roux and Karplus, 1991a; Roux and Karplus, 1995), and the treatment of the polarization energy through second order (Roux, 1993). Estimated free energies were corrected for finite size effects by using a continuum electrostatic reaction field approximation. Because the ion binding sites are very distant (more than 18 Å apart), particular attention was given to the treatment of long range electrostatic interactions. To describe the electrostatic forces realistically at all distances it was necessary to avoid the truncation with switching functions used in most simulations (Brooks et al., 1983). Instead, a finite system with no cutoff was chosen to model the gramicidin channel. To decrease the computational time, the long range interactions were evaluated with the extended electrostatics procedure (see Theory and Methodology for details) (Brooks et al., 1983; Stote et al., 1991).

In the next section, the definition of the free energy of single and double occupancy is introduced and related to the phenomenological Eyring rate theory models, and the microscopic model, potential function, and the free energy calculations are described. The main results are described and discussed and a concluding discussion of the results is given.

THEORY AND METHODOLOGY

Free energy of single and double occupancy

The ion-gramicidin channel system can be treated in terms of four states: the unoccupied channel, the singly occupied channel with an ion in the left

binding site, the singly occupied channel with an ion in the right binding site, and the doubly occupied channel with ions in both binding sites. Although the distinction between the right and left well is not essential to describe the equilibrium states of a symmetric dimer channel, it is closely related to phenomenological barrier-hopping models based on rate theory used to describe the flux going through the channel in the presence of an applied membrane voltage (see below). To describe the thermodynamics of single and double occupancy, we defined the free energy of the unoccupied channel $\mathcal{A}[0, 0]$, the free energy of the singly occupied channel $\mathcal{A}[i, 0] = \mathcal{A}[0, i]$, and the free energy of the doubly occupied channel $\mathcal{A}[i, i]$. The relative free energy of binding one ion i in the singly occupied state is

$$\Delta\mathcal{A}_i^S = \mathcal{A}[0, i] - \mathcal{A}[0, 0], \tag{1}$$

and the relative free energy of binding a second ion in the doubly occupied state is

$$\Delta\mathcal{A}_i^D = \mathcal{A}[i, i] - \mathcal{A}[i, 0]. \tag{2}$$

We do not consider the case where there are two different ions in the doubly occupied channel. The relative free energy of the singly and doubly occupied states can be related to the phenomenological transition rate constants used to describe the ion fluxes in the gramicidin channel, e.g., the kinetic diagram of the 3B2S2I model of Andersen shown in Fig. 1 (the acronym 3B2S2I means 3 barriers, 2 sites, and 2 ions; see the caption for details) (Becker et al., 1992). In particular, the association constant of an ion to the left binding site while the right site is unoccupied is (binding constant in the given singly occupied state)

$$K_i^S = \frac{k_{[0,0]\to[i,0]}}{k_{[i,0]\to[0,0]}} = K_0 \exp\left(-\frac{\Delta\mathcal{A}_i^S}{k_B T}\right), \tag{3}$$

and the association constant of an ion to one site while the other site is occupied (binding constant in the doubly occupied state) is

$$K_i^D = \frac{k_{[0,i]\to[i,i]}}{k_{[i,i]\to[0,i]}} = K_0 \exp\left(-\frac{\Delta\mathcal{A}_i^D}{k_B T}\right), \tag{4}$$

where K_0 is a constant standard state factor involving the translational partition function of the ion (McQuarrie, 1976). If there were no coupling between the two ions in the binding sites of the channel, the two binding constants K_i^D and K_i^S would be equal. The actual free energy of binding one ion in the doubly occupied state relative to the singly occupied state is

$$\Delta\mathcal{A}_i^{SD} = -k_B T \ln\left[\frac{K_i^D}{K_i^S}\right], \tag{5}$$

where

$$\begin{aligned}\Delta\mathcal{A}_i^{SD} &= \Delta\mathcal{A}_i^D - \Delta\mathcal{A}_i^S \\ &= (\mathcal{A}[i, i] - \mathcal{A}[0, i]) - (\mathcal{A}[0, i] - \mathcal{A}[0, 0]) \\ &= \mathcal{A}[i, i] - 2\mathcal{A}[0, i] + \mathcal{A}[0, 0],\end{aligned} \tag{6}$$

and corresponds to a measure of ion-ion interactions inside the channel. In the variation of $\Delta\mathcal{A}_i^{SD}$ for different type of ions i and j, the free energy of the unoccupied channel cancels, so that

$$\begin{aligned}\Delta\Delta\mathcal{A}_{ij}^{SD} &= \Delta\mathcal{A}_j^{SD} - \Delta\mathcal{A}_i^{SD} \\ &= (\mathcal{A}[j, j] - \mathcal{A}[j, 0] - \mathcal{A}[0, j]) - (\mathcal{A}[i, i] - \mathcal{A}[i, 0] - \mathcal{A}[0, i]) \\ &= (\mathcal{A}[j, j] - \mathcal{A}[i, i]) - 2(\mathcal{A}[j, 0] - \mathcal{A}[i, 0]) \\ &= \Delta\mathcal{A}_{ij}^D - 2\Delta\mathcal{A}_{ij}^S.\end{aligned} \tag{7}$$

The quantities $\Delta\mathcal{A}_{ij}^D$ and $\Delta\mathcal{A}_{ij}^S$ represent free energy differences for the alchemical transformation from ion of type i to ion of type j in the doubly and singly occupied states, respectively. Both free energy differences can be calculated with standard free energy perturbation or thermodynamic integration techniques from simulations in which the occupancy of the channel does not change (Berendsen et al., 1982; Gao et al., 1989; Singh et al., 1987; Straatsma and Berendsen, 1988). These computational methodologies are now well documented. Briefly, the free energy difference between two microscopic systems with potential energy $U(1)$ and $U(2)$ is calculated from an ensemble average generated with system 1 (Zwanzig, 1954)

$$\mathcal{A}_2 - \mathcal{A}_1 = -k_B T \ln\left\langle \exp\left(-\frac{U(2) - U(1)}{k_B T}\right)\right\rangle_{(1)}, \tag{8}$$

or from an equivalent ensemble average generated with system 2. In actuality, if the changes between $U(1)$ and $U(2)$ are not very small, it is better to use a set of intermediate parameters, λ_i, so that Eq. 8 becomes

$$\mathcal{A}_2 - \mathcal{A}_1 = \sum_{i=1}^{n-1} -k_B T \ln\left\langle \exp\left(-\frac{U(\lambda_{i+1}) - U(\lambda_i)}{k_B T}\right)\right\rangle_{(\lambda_i)}, \tag{9}$$

with $U(\lambda_1) = U(1)$ and $U(\lambda_n) = U(2)$. In the limit of a large number of very small perturbations, Eq. 9 is equivalent to the thermodynamic integration formula (Kirkwood, 1935)

$$\mathcal{A}_2 - \mathcal{A}_1 = \int_{\lambda_1}^{\lambda_2} d\lambda \left\langle \frac{\partial U}{\partial \lambda}\right\rangle. \tag{10}$$

In the present calculations, the perturbations correspond to the charge of a Na^+ or the nonbonded van der Waals and core parameters of Li^+, Na^+, K^+, Rb^+, and Cs^+. The free energy differences were calculated stepwise, with small perturbations, by using Eq. 9, e.g., to transfer the van der Waals parameters of one ion into those of another (see below).

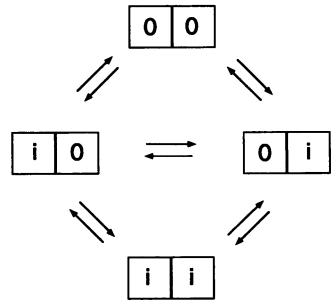

FIGURE 1 The rate theory 3B2S2I model with 3 barriers, 2 sites, and 2 ions used by Andersen to analyze voltage-flux measurements with the gramicidin channel (Becker et al., 1992). The transition rate constants between the different states are not indicated on the diagram for the sake of clarity. In the text, they are expressed explicitly in terms of the initial and final states, e.g., the transition rate constant between the water-filled unoccupied channel (state [0,0]) to the singly occupied channel with one ion i on the left site (state [i,0]) is $k_{[0,0]\to[i,0]}$. The other rates are expressed similarly.

Microscopic model and potential function

The gramicidin channel was constructed as a right-handed head-to-head dimer from the coordinates determined experimentally by use of proton-proton nuclear Overhauser effect (NOE) distances (Arseniev et al., 1985; Arseniev et al., 1986). The procedure used is that described in Roux and Karplus, 1993. We briefly summarize the method here. The primary solvation of the channel structure was provided by building 24 water molecules into the structure; there are 12 water molecules along the pore axis separated by a distance of 2.8 Å and 6 at each extremity of the channel. The axis of the channel is oriented along x. Hemispherical bulk-like water regions were constructed by overlaying water molecules taken from the coordinates of a pure water sphere of radius 10 Å equilibrated at 300 K and deleting the water molecules overlapping with the channel or the first 24 waters. To produce a hydrocarbon-like environment and to prevent waters from reaching the lateral side of the dimer, a model membrane is included. A similar overlay method is used to construct the model membrane made of Lennard-Jones

spheres (no charge or polarizability) corresponding to the size of a CH_3 group (r_{min} = 2.165 Å, ϵ = −0.1811 kcal/mol). All heavy atoms and all polar hydrogens (those able to form hydrogen bonds) are included. The aliphatic hydrogens are treated as part of the carbon to which they are attached in an extended atom model. The initial water-filled channel system consists of 314 peptide atoms for the gramicidin dimer, 190 TIP3P water molecules (Jorgensen et al., 1983) and 85 Lennard-Jones spheres. Approximately 10 water molecules are located inside the channel, and 90 waters are in hemispherical caps at each mouth of the channel.

To construct the system in the singly and doubly occupied state, one water molecule located near ±9.2 Å at the position of the ion binding site as determined from a previous calculation (Roux and Karplus, 1993) was substituted by a Na^+ ion. Six water molecules are located inside the channel between the two ions in the doubly occupied state. This number was determined from the average diameter of a water molecule, 2.8 Å, and the position of the Na^+ binding sites in a linear configuration. Assuming that the water molecules nearest to the cation are 2.2 Å away from the ion, at ±7.0 Å, and that the water-water distance is 2.8 Å, the maximum number of internal waters is (9.4 + 9.4 − 2.2 − 2.2)/2.8 + 1 = 6, i.e., the approximate position of the six internal waters along the channel axis is ±7.0, ±4.2, and ±1.4 Å, although the ions, the water and all the atoms of the channel are free to move during the simulation. In the present investigation it is assumed that the number of water molecules between the two ions in the doubly occupied state does not vary with ion type. There are ~1000 particles in the channel system for the three occupancy states. The main feature of the simulation system and its dimensions are illustrated schematically in Fig. 2.

The water-water (TIP3P) (Jorgensen et al., 1983), peptide-peptide (CHARMM) (Brooks et al., 1983), water-peptide (Reiher, 1985; Reiher and Karplus, unpublished results, 1985), and ion-peptide (Roux and Karplus, 1991a; Roux and Karplus, 1995) potential functions used have been described elsewhere. Special care was given to the parameterization of the interaction of the cations with the channel and water. In a previous ab initio study (Roux and Karplus, 1995), it was found that standard Lennard-Jones 6–12 potential functions with fixed charges could not reproduce the energies and optimized geometry for the cations interacting with *N*-methylacetamide, taken as model of the peptide backbone; e.g., the cation-peptide interaction energy is underestimated by approximately 10, 6, and 4 kcal/mole for Li^+, Na^+, and K^+ ions, respectively. This tendency was indicative of the increasing ion-induced polarization energy for the smaller cations in their interactions with the peptide group.

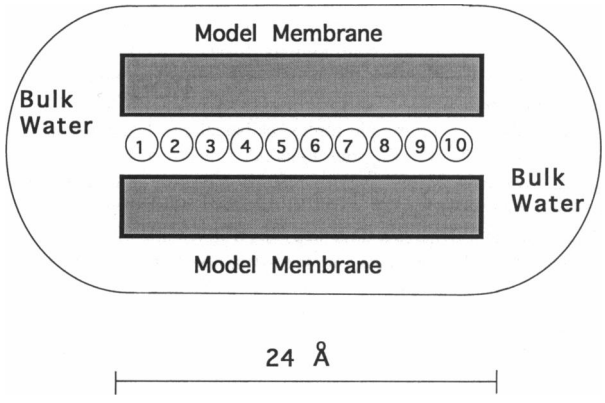

FIGURE 2 Schematic representation of the gramicidin A dimer system. The water-filled channel system consists of 314 peptide atoms for the gramicidin dimer, 190 TIP3P (Jorgensen et al., 1983) water molecules (10 single file and 90 in each spherical cap) and 85 Lennard-Jones model membrane spheres; there are 969 particles. A spherical boundary potential given by Eq. 16 is applied on the water molecules in each cap; a similar planar potential and a cylindrical potential given by Eq. 17 are applied to the Lennard-Jones spheres. A Na^+ ion was substituted for water number 2 to construct the singly occupied channel system; a second Na^+ ion was substituted for water number 9 to construct the doubly occupied channel system. There are 6 water molecules located between the two ions in the doubly occupied state.

The interactions involving the ions is given by

$$E_{i\text{-}c} = E_{core} + E_{vdW} + E_{elec} + E_{pol}, \quad (11)$$

where E_{core} is the core repulsion $A^{(8)}/r^8$, E_{vdW} is the van der Waals attraction $-B^{(6)}/r^6$, E_{elec} is a standard electrostatics interaction between the ion and the partial charge of the peptide atoms, and E_{pol} is an ion-induced polarization interaction. The short range ion-carbonyl oxygen core repulsion E_{core}, represented by a $\sim 1/r^8$ energy term, is softer than the more standard $\sim 1/r^{12}$ repulsion of the Lennard-Jones 6–12 potential.

All of the ion interaction parameters used in the calculation are reported in Tables 1 and 2; polarizability coefficients and other parameters have been given elsewhere (Roux and Karplus, 1991a). The other van der Waals Lennard-Jones 6–12 interactions parameters (Brooks et al., 1983) and the electrostatic partial charges used in E_{elec} have been taken from previous work (Reiher, 1985; Reiher and Karplus, unpublished results, 1985). The parameters $A^{(8)}$ and $B^{(6)}$ of Li^+, Na^+, and K^+ were adjusted to fit calculated ab initio potential energy surfaces (Roux and Karplus, 1995). Equivalent ab initio surfaces are not available for Rb^+ and Cs^+ and the core size and well depth parameters of those ions were developed empirically. The relative differences in ionic radii for the different cations, as defined by Pauling (Pauling, 1960) and by Gourary-Adrian (Gourary and Adrian, 1960), were used to estimate the position of the optimal cation-ligand distance that should be reproduced by the potential function. Such a relation of ionic radii with optimized geometries is supported by ab initio calculations of Li^+, Na^+, and K^+ with *N*-methylacetamide and water (see Tables 1, 2, and 3). On the basis of this argument, the optimal Rb^+- and Cs^+-ligand distance should be approximately 0.2 Å and 0.4 Å, respectively, greater than for K^+. For example, the optimal distance should be 2.88 Å with carbonyl oxygen and 2.99 Å with water oxygen in the case of Cs^+. However, the Pauling ionic radii are not sufficient to deduce both the position and the depth of the energy minimum of the potential function for Rb^+ and Cs^+. To supplement the information available from the ionic radii, it is assumed that the free energy of an ion inside the channel is equal to the experimental free energy of solvation of this ion in bulk water. On the basis of the equilibrium cation binding constants (Hinton et al., 1986; Hinton et al., 1988), the free energy of the ions in the channel binding site can be taken to be the free energy of solvation in bulk water to a good approximation. For example, the final parameters $A^{(8)}$ and $B^{(6)}$ for Rb^+ were adjusted to yield simultaneously a free energy difference of approximately 5 kcal/mol relative to K^+ for the ion in the channel binding site (based on the experimental solvation free energy of K^+ and Rb^+ in bulk water) and a carbonyl oxygen distance of 2.68 Å in the optimized complex of the ion with *N*-methylacetamide (based on the ionic radii of K^+ and Rb^+). The parameters for Cs^+ were developed in a similar fashion.

Except for the polarization term E_{pol}, Eq. 11 is a standard nonbonded empirical potential energy function of the type used generally in computer simulations of macromolecular systems (Brooks et al., 1988). However, the van der Waals functional form is unusual. Most theoretical studies of biomolecular systems are based on pairwise additive nonbonded interatomic

TABLE 1 Ion-N-methylacetamide interaction energies

Ion	A_8 (kcal/mol) Å^8	B_6 (kcal/mol)Å^6	Distance* (Å)		Energy (kcal/mol)
Li^+	2,750	−150	1.81		−51.4
				(0.29)	
Na^+	6,200	−290	2.10		−37.8
				(0.39)	
K^+	30,000	−3600	2.49		−30.4
				(0.19)	
Rb^+	54,500	−6350	2.68		−27.4
				(0.20)	
Cs^+	100,000	−11000	2.88		−24.9

*Difference between adjacent pairs of ion-ligands are shown in parentheses for comparison with Pauling and Gourary-Adrian radii; see text.

TABLE 2 Ion-water potential function

Ion	A_{12} (kcal/mol)Å^{12}	B_6 (kcal/mol)Å^6	Distance* (Å)	Energy‡(kcal/mol) Calculated	Energy‡(kcal/mol) Experimental
Li^+	18,000	−270	1.88	−36.9	−34.0
			(0.32)		
Na^+	82,965	−440	2.20	−27.4	−24.0
			(0.41)		
K^+	478,002	−800	2.61	−19.6	−17.9
			(0.17)		
Rb^+	845,240	−777	2.78	−17.2	−15.9
			(0.22)		
Cs^+	1,868,503	−1241	3.00	−15.1	−13.7

*Difference between adjacent pairs of ion-ligands are shown in parentheses for comparison with Pauling and Gourary-Adrian radii in Table 3.
‡Gas phase data are taken from Džidić and Kebarle, 1970.

TABLE 3 Empirical ionic radii (Å)*

Ion	Pauling‡	Gourary-Adrian§
Li^+	0.60	0.94
	(0.35)	(0.23)
Na^+	0.95	1.17
	(0.38)	(0.32)
K^+	1.33	1.49
	(0.15)	(0.14)
Rb^+	1.48	1.63
	(0.21)	(0.23)
Cs^+	1.69	1.86

*Difference between adjacent pairs of ion-ligands are shown in parentheses for comparison with Tables 1 and 2.
‡ Taken from Pauling, 1960.
§ Taken from Gourary and Adrian, 1960.

potential energy functions in which it is assumed that many-body effects are negligible or can be accounted for by an effective pairwise additive function (Brooks et al., 1988). Although this assumption appears to be a good approximation in systems involving neutral solutes and proteins (Goodfellow, 1982; van Belle et al., 1987), it is violated when small ions are present because the strong ion-ligand interactions can give rise to significant many-body effects (Clementi et al., 1980; Dang et al., 1991; Roux, 1993). In the present study, a standard empirical energy function complemented by ion-induced polarization and many-body effects, was used. In a previous study, nonadditive second order polarization energy was found necessary to obtain the correct magnitude for the absolute free energy of Na^+ in the channel; its contribution amounts to almost 40% of the total free energy (see appendix) (Roux, 1993). Because the water and peptide potential functions have been developed as effectively pairwise additive (Brooks et al., 1983; Jorgensen et al., 1983; Reiher, 1985; Reiher and Karplus, unpublished results, 1985), with nonadditive many-body effects incorporated in an average sense, only the ion-induced polarization is included. The induced dipole on atom i by the charge q_{ion} of the ion is

$$\mu_i = \alpha_i q_{ion} \frac{(r_i - r_{ion})}{|r_i - r_{ion}|^3}, \tag{12}$$

where α_i is the atomic polarizability of atom i. The polarizabilities α_i of the peptide atoms were chosen to reproduce the ab initio calculations (Roux and Karplus, 1995), and their values are similar to other atomic polarizabilities (Brooks et al., 1983). No polarizability was attributed to the water molecules because the interactions of singly charged ions with water can be reasonably well described with standard fixed charge models (Jorgensen and Severance, 1993). In the present approximation, the polarization interaction E_{pol} arises from the interaction between the point dipole induced on the peptide atoms by the ion and all the other charges in the system (Dang et al., 1991; Goodfellow et al., 1982; Lybrand and Kollman, 1985; van Belle et al., 1987).

To first order, the dipole μ_i induced on atom i interacts with the charge of the ion according to the expression

$$E_{pol}^{(1)} = -\frac{1}{2}\sum_i \frac{\mu_i(r_i - r_{ion})}{|r_i - r_{ion}|^3} q_{ion} = -\frac{1}{2}\sum_i \frac{\alpha_i q_{ion}^2}{|r_i - r_{ion}|^4}. \tag{13}$$

To second order, the induced dipoles interact with all other charges q_j in the system

$$E_{pol}^{(2)} = \sum_{ij} -\frac{\mu_i (r_i - r_j)}{|r_i - r_j|^3} q_j. \tag{14}$$

Both first and second order polarization were included in the present calculations. The first order polarization $E_{pol}^{(1)}$ which was included in previous studies of the gramicidin channel (Roux and Karplus, 1991a; Roux and Karplus, 1991b; Roux and Karplus, 1993), results in a pairwise additive attractive interaction. The second order term $E_{pol}^{(2)}$, representing a non-pairwise-additive contribution to the potential energy function, results in an effective reduction of the ion affinity for the backbone carbonyl groups of the channel (Roux, 1993). From a computational point of view the present approximation is advantageous because the induced polarization is not calculated self-consistently with an iteration procedure (i.e., the electric field created by the induced dipoles does not influence other induced dipoles) in contrast with other treatments (Dang et al., 1991; van Belle et al., 1987). Although this represents an approximation, it has been shown by comparison with ab initio calculations that the second order approximation retains the dominant nonadditive contributions (Roux, 1993). Straatsma and McCammon have also used such an approximate polarizability correction in a treatment of water (Straatsma and McCammon, 1990).

To describe the microscopic forces realistically at large distances it is necessary to avoid truncating the nonbonded electrostatic interactions in the usual way with switching functions. As the finite gramicidin system contains ~1000 atoms, an explicit sum over all nonbonded pairs with no truncation at each dynamics time step would be computationally prohibitive. The extended electrostatics method (Brooks et al., 1983; Stote et al., 1991) was used to compute the complete interaction within a normal cutoff (12 Å) and to add the interaction between the given atom and dipoles and quadrupoles of predefined groups outside this cutoff. This allows the long range interactions to be computed in a reasonable time, it requires ~50% longer than the standard nonbonded interactions computed with a cutoff of 12 Å. This simple procedure for avoiding the need for truncation is similar in spirit to the fast multipole methods developed more recently (Shimada et al., 1994).

Computational details and simulation procedure

The center of mass of the dimer was placed at the origin, and the channel axis, defined as the line going through the center of mass of each monomer, is oriented along the x axis. To maintain the orientation of the channel in

the finite system a harmonic restraining potential

$$E_{\text{restraint}} = \frac{k}{2}(X_{\text{cm}}^2 + Y_{\text{cm}}^2 + Z_{\text{cm}}^2) + \frac{k}{2}(Y_{\text{cm1}}^2 + Z_{\text{cm1}}^2) + \frac{k}{2}(Y_{\text{cm2}}^2 + Z_{\text{cm2}}^2), \qquad (15)$$

where the coordinates cm, cm1, and cm2 refer to the center of mass of the dimer and of monomers 1 and 2, respectively. A value of $k = 1000$ kcal/mol/Å was used. Although a similar configurational restriction was achieved with holonomic constraints by using SHAKE (Ryckaert et al., 1977) in the previous calculation of the free energy profile of Na^+ (Roux and Karplus, 1993), an approach based on restraining potentials was chosen here because it is generally easier to implement in the molecular dynamics algorithm. A hemispherical potential, similar to that used in stochastic spherical boundary simulations (Brooks and Karplus, 1983), was applied on the water oxygen to confine the water caps at each mouth of the channel

$$E_{\text{caps}} = \begin{cases} 0.2\, d^2\,(d^2 - 2.25) & \text{for} \quad d > 0 \\ 0 & \text{otherwise,} \end{cases} \qquad (16)$$

where d is $|r - r_0| - \Delta r$, r is the oxygen position of the water molecule, $r_0 = (\pm 8, 0, 0)$, $\Delta r = 13$. A planar potential, similar to Eq. 16 was applied in the x direction to the Lennard-Jones model membrane spheres to prevent their diffusion into the bulk water region. A half-harmonic cylindrical potential was applied to the Lennard-Jones spheres in the radial direction perpendicular from the x axis

$$E_{\text{cyl}} = \begin{cases} (r - 11.5)^2 & \text{for} \quad r > 11.5 \\ 0 & \text{otherwise,} \end{cases} \qquad (17)$$

where $r^2 = (y^2 + z^2)$.

The water-filled channel was first equilibrated for 25 ps and a trajectory of 100 ps was generated. The water molecule nearest to the binding site was substituted by a Na^+ to construct the singly occupied state and the system was equilibrated for 10 ps followed by a production run of 50 ps including first and second order polarization energy. The doubly occupied state was then constructed from a similar substitution for the water molecule nearest to the other binding site. After a short initial energy minimization, the system was equilibrated for 10 ps followed by a second production run of 50 ps. Other cations were substituted for the Na^+ ions to obtain singly and doubly occupied states. These were followed by similar equilibration and production trajectories. Trajectories of 50 ps were generated to calculate the free energy of charging a Na^+ in the singly and doubly occupied channel states (see details below).

The relative free energy differences were calculated on the basis of Eq. 8 from the trajectories of the five normal cations. Four ions with intermediate Lennard-Jones and core parameters obtained from a linear interpolation of the parameters of the five normal cations, were used to perform the free energy calculations by Eqs. 8 and 9. Both forward and backward simulations were performed. A similar approach was used to calculate the relative free energies in the doubly occupied states. In addition, the free energy associated with the process of charging the Na^+ ion in the singly and doubly occupied states relative to the corresponding neutral van der Waals sphere was calculated with a similar approach by using the free energy perturbation method (Straatsma and Berendsen, 1988). Ten trajectories were generated with a Na^+ charge of 0.95, 0.05, 0.85, $\cdots$, 0.05, and the free energy differences were calculated by perturbating the charge by ± 0.05. For each window, the system was equilibrated for 2.5 ps and a trajectory of 2.5 ps was generated; the complete calculation of the free energy of charging for one occupancy state is equivalent to a single trajectory of 50 ps. For the free energy of charging in the doubly occupied state, ten trajectories were generated with a similar procedure with the charge of one Na^+ taking values of 0.95, 0.05, 0.85, $\cdots$, 0.05 while the charge of the second Na^+ remained equal to one. During the charging calculations, the ions had a tendency to leave the channel when their charge was smaller than $0.25e$ due to the decrease in ion-channel interactions. To maintain the Na^+ in the channel binding site during the charging free energy calculations, the ions were constrained at $x = 9.4$ Å along the channel axis by using a harmonic potential with a strong force constant of 500 kcal/mol/Å^2; no constraint was applied in the other two directions, and the ions were free to move in y and z. No such constraint was used in the relative free energy calculations in the singly and doubly occupied states. As their charge is not altered during those calculations the ions remain in the channel binding site.

To compare with the free energy of Na^+ in the channel, a spherical system containing 250 water molecules was constructed and the bulk solvation properties of the model cations were calculated. The number of waters in the spherical system was chosen in accord with the size of the water caps used in the channel simulations. A spherical boundary potential, similar to Eq. 16 was used with $r_0 = (0, 0, 0)$ and $\Delta r = 12$. A water sphere was constructed around a central Na^+ with an equilibrated pure water system. The simulation system was equilibrated for 10 ps and a trajectory of 50 ps was generated. The nonbonded interactions were treated with the extended electrostatic method and were not truncated.

Free energy calculations in which the net charge is modified, in contrast to those comparing two ions with the same charge, are strongly influenced by the finite size of the simulation system. To obtain meaningful results, it is necessary to estimate the magnitude of the free energy contribution of distant parts of the system that are not present in the microscopic model. One possibility is to represent the empty space around the microscopic system by a continuum dielectric. Procedures similar in spirit have been used to account for truncating the electrostatic interactions in calculating the chemical potential of ions (Åqvist, 1990). The finite size correction for the charging free energy of Na^+ inside the sphere of 250 water molecules can be obtained by the Born charging expression (Born, 1920; Roux et al., 1990; Straatsma and Berendsen, 1988),

$$E_{\text{rf}} = -\frac{1}{2}\frac{Q^2}{R}\left[1 - \frac{1}{\epsilon}\right], \qquad (18)$$

where Q is the ion charge, ϵ is the dielectric constant of the surrounding continuum, and R is the radius of the sphere. Other cations were substituted for the Na^+ ion followed by similar equilibration and production trajectories. In all the simulations the ion was kept in the center of the sphere. The relative free energy differences in the water sphere were calculated from the trajectories of the five normal cations by using four ions with intermediate parameters obtained from a linear interpolation of their van der Waals parameters, as described for the calculations in the channel system. Similarly, the charging free energy of Na^+ in the water sphere was calculated by using the free energy perturbation method with 10 windows, resulting in a 50-ps trajectory. The simple Born charging expression Eq. 18 does not provide a valid estimate of the finite size correction that is needed in the case of the channel calculations because the ion sites are not located near the center of the simulation system. A more general expression is provided by the multipolar expansion for the reaction field acting on the charge distribution inside a spherical region embedded in a dielectric continuum derived by Kirkwood (Kirkwood, 1934)

$$E_{\text{rf}} = -\frac{1}{2}\sum_{lm}\frac{4\pi |Q_{lm}|^2}{(2l+1)}\frac{1}{R^{2l+1}}\left[\frac{\epsilon - 1}{\epsilon + l/(l+1)}\right], \qquad (19)$$

where Q_{lm} are the electrostatic multipoles, ϵ is the dielectric constant of the surrounding continuum, and R is the radius of the cavity. In the case of an ion at the center of a spherical system, all the multipoles vanish except the monopole Q_{00} and Eq. 19 reduces to the Born expression Eq. 18. Eq. 19 was used to obtain a finite size correction for the free energy of the singly and doubly occupied states in the channel.

In all the simulations with the singly and doubly occupied channel systems, the hydrocarbon-like Lennard-Jones spheres, the oxygens of the water molecules in the bulk-like regions, and the side chains of the channel were submitted to dissipative and stochastics Langevin forces corresponding to a velocity relaxation rate of 40 ps^{-1}; this value is appropriate for the diffusion of a water molecule (Brunger et al., 1984). It was introduced to obtain better convergence of the Boltzmann statistics characteristic of a canonical ensemble. In the simulations based on the spherical water system, the water oxygens were submitted to similar dissipative forces. First and second order polarization was included in all the calculations for the channel system. No ion-induced polarization was included in the simulations with the water

TABLE 4 Charging free energies of Na^+

Perturbations	Free energy (kcal/mol) Singly occupied	Doubly occupied	Water sphere
Charging	−100	−81	−95
Finite size correction*	−7	−20	−14
Total	−107	−101	−109

*The finite size correction for the water sphere is based on Eq. 18 and those for the channel are based on Eq. 19; see text.

TABLE 5 Relative free energies (kcal/mol)

Perturbations	Singly occupied gramicidin A	Doubly occupied gramicidin A	Water sphere
Li^+ to Na^+	24.4	46.4	21.6
Na^+ to K^+	14.4	27.2	24.9
K^+ to Rb^+	6.2	12.9	9.2
Rb^+ to Cs^+	6.3	12.4	6.4

sphere system for reasons already given. The integration time step was 0.001 ps for the dynamics. The results of all of the free energy calculations are given in Tables 4, 5, 6, and 7.

RESULTS AND DISCUSSION

Structural aspects

In all the molecular dynamics trajectories the channel structure remains very close to the initial right-handed conformation; the average difference with the initial structure is on the order of 1.0 Å and fluctuations of the backbone atoms around the mean structure are on the order of 0.5 Å. The water molecules located inside the channel maintained a single file arrangement with an average linear spacing of $\sim 2.8 \pm 0.15$ Å as observed in a simulation of the left-handed helical dimer with a similar model membrane (Roux, 1995). The cations remained in their binding sites in both the trajectories of the singly and doubly occupied states. However,

TABLE 6 Cation free energies (kcal/mol)*

Ions	Bulk water Experimental‡	Calculated§	Singly occupied gramicidin A Calculated
Li^+	−123.5 (25.2)	−130 (21.6)	−131 (24.4)
Na^+	−98.3 (17.5)	−109 (24.9)	−107 (14.4)
K^+	−80.8 (4.2)	−84 (9.2)	−92 (6.2)
Rb^+	−76.6 (5.6)	−75 (6.4)	−86 (6.3)
Cs^+	−71.0	−68	−80

*All of the calculated values were deduced from the charging free energy of Table 5 and the relative free energies of Table 6 obtained for Na^+ in the water sphere and in the singly occupied channel.

‡ Experimental values are taken from Friedman and Krishnan, 1973.

§ Calculated from the sphere of 250 TIP3P water molecules; see text.

TABLE 7 Double occupancy free energy

Ion	Free energy contributions (kcal/mol)* $\Delta\Delta A^{SD}$	Internal H_2O	Carbonyl oxygens
Li^+	0.0	0.0	0.0
Na^+	−2.4	−1.9	0.1
K^+	−3.8	−4.9	1.4
Rb^+	−3.3	−5.6	2.5
Cs^+	−3.6	−5.9	3.2

*All free energies are given relative to Li^+.

it was observed during the parameterization of the Rb^+ and Cs^+ that the average position of those ions was sensitive to the value of the carbonyl core $A^{(8)}$ and the van der Waals $B^{(6)}$ parameters used in Eq. 11. In some preliminary cases, the ion left the channel to go into the bulk water region. Nevertheless, all of the ions were finally stable in the binding site after the parameters were optimized with respect to the core size, taken from the Pauling radius, and relative free energy of solvation, taken from the free energy of solvation in bulk water. The optimized parameters are reported in Table 1 (see also the discussion in the previous section). The average position of the binding site for the five cations are given in Table 8 for the singly and doubly occupied states (the root mean square (rms) fluctuations are given in parentheses). The averages are approximately independent of ion type although the results are not identical. Also, there is a small difference between the two ions in the doubly occupied state with the second distance being slightly smaller than the first in all cases (except for Li^+). Analysis of the structures suggests that this asymmetry in the average ion position is caused by a slightly different conformation of the backbone near the Trp side chains. The Trp side chains are in direct contact with the nonpolar Lennard-Jones spheres surrounding the channel and it is likely that their average conformation is not described realistically by the present model membrane. In a real system, the averages should be symmetric, although asymmetric results could occur at specific times. Studies based on more realistic models of the phospholipid membrane will be necessary to answer questions about the influence of the environment on the channel. Work is currently in progress on this subject (Woolf and Roux, 1993; Woolf and Roux, 1994).

TABLE 8 Average ion position along channel axis (Å)*

Ions	Singly occupied	Doubly occupied
Li^+	8.44 (0.25)	9.67 (0.24) −8.64 (0.21)
Na^+	9.45 (0.24)	9.33 (0.23) −9.06 (0.20)
K^+	9.31 (0.17)	9.45 (0.28) −9.15 (0.31)
Rb^+	8.92 (0.26)	9.08 (0.55) −9.27 (0.43)
Cs^+	8.62 (0.57)	8.63 (0.27) −8.61 (0.21)

*Zero is at the center of the dimer channel (see Fig. 2 for definition). The rms fluctuations are given in parentheses.

Although the present calculations, which are based on a simplified model membrane, cannot provide more quantitative information about this, they do indicate that the positions of the binding sites are sensitive to the conformation of the side chains.

Charging free energy for Na^+ in the channel and in water

Details of the various contributions to the charging free energies of Na^+ in the bulk water and in the singly and doubly occupied gramicidin channel are given in Table 4. The calculated charging free energy for Na^+ is -95 kcal/mol in the bulk water sphere and -100 and -81 kcal/mol in the singly and doubly occupied channel states, respectively. With a radius of 12 Å and a dielectric constant of 78.4, a correction of -14 kcal/mol is obtained on the basis of Eq. 18. This results in a total charging free energy of -109 kcal/mol for Na^+ in bulk water. Nonadditive second order polarization energy was included in the channel calculations, as described in Theory and Methodology. It is essential to obtain the correct magnitude for the absolute free energy of Na^+ in the channel. Free energy calculations described in the Appendix show that the contribution of the second order interactions between the ion-induced dipoles on the peptide and the fixed partial charges in the system is 40–45 kcal/mol for Na^+. However, approximations based on first order polarization are expected to remain valid in the calculation of the relative free energy profile along the channel axis (potential of mean force) due to a cancellation of the large contribution of the second order term (Roux and Karplus, 1991a; Roux and Karplus, 1991b; Roux and Karplus, 1993; Watanabe et al., in preparation).

The finite size correction to the charging free energy for the singly and doubly occupied states was calculated on the basis of Eq. 19 with a radius of 22 Å for the spherical cavity, obtained from the distance of the farthest water, and a value of ϵ of 78.4, corresponding to bulk water. The multipoles from $l = 0$–40 were included in the sum. The finite size corrections to the charging free energy of one Na^+ in the channel are -7 and -20 kcal/mol for the singly and doubly occupied channel states, respectively. The resulting total free energies of Na^+ are -107 and -101 kcal/mol. The magnitude of the finite size correction for the doubly occupied channel (-20 kcal/mol) is approximately equal to three times the value for the singly occupied channel (-7 kcal/mol). This is due to the fact that the correction depends quadratically on the magnitude of the multipoles and that the sum in Eq. 19 is dominated by the contribution of the monopole ($l = 0$ corresponds to the total charge); i.e., the correction varies approximately as $2^2 - 1^2$ in going from a singly to a doubly charged system.

Use of a spherical cavity and the neglect of the low dielectric constant medium (the electrostatic reaction field expression based on Eq. 19 ignores the difference in the dielectric constants of the bulk water and bilayer membrane that are outside a radius of 22 Å) is clearly an approximation. Nevertheless, the spherical cavity is related to a possible physical situation. In effect, the microscopic model with the finite size correction based on Eq. 19 treats the system as if the channel was embedded in a hydrophobic spherical micelle of 22 Å radius (the region of space occupied by the neutral membrane-like Lennard-Jones spheres in the atomic model corresponding to a low dielectric, where $\epsilon = 1$). To incorporate the influence of the planar dielectric discontinuity arising from the membrane, a treatment based on a numerical solution of the Poisson-Boltzmann equation with a discrete grid would be necessary (Gilson and Honig, 1988). The spherical cavity approximation was chosen because it leads to an analytic expression for the finite size correction.

The purpose of calculating the charging free energies here is not to obtain quantitative results but rather to determine whether the empirical energy function gives qualitatively correct values. The calculated free energy in bulk water (-109 kcal/mol) is slightly larger in magnitude than the experimental estimate of the chemical potential of Na^+ in water (Friedman and Krishnan, 1973) (-98.3 kcal/mol). The charging free energy reported here does not include the reversible work needed to create the cavity to insert a neutral Na^+ in the system. Although these contributions are expected to be small (on the order of $+2$ to $+3$ kcal/mol) (Jorgensen et al., 1989), their evaluations would require very long simulations to account properly for the relaxation of the water molecules. This is particularly important for the single file water molecules inside the channel that have very long relaxation times (Chiu et al., 1991; Roux, 1995). An alternate approach consists of calculating the relative free energy difference between a water molecule and the neutral Na^+ in the channel binding site and in the bulk water region (Åqvist and Warshel, 1989).

The charging free energy of a second Na^+ in the doubly occupied channel is -101 kcal/mol, slightly less negative than the charging free energy of the Na^+ in the singly occupied channel (-107 kcal/mol) due to the effective ion-ion repulsion. It should be stressed that the bare ion-ion repulsive interaction is on the order of $+18$ kcal/mol in vacuum. In the channel environment, this repulsion is reduced to $+6$ kcal/mol due to the polarization of the surrounding environment. The calculation includes only the ion repulsion due to the charging free energy and the free energy for cavity formation has been neglected. According to experimental estimates, the value of 6 kcal/mol is of the correct order but somewhat too large (Becker et al., 1992). The residual repulsion corresponds to an effective dielectric constant of 2.6. This is due to the fact that the water molecules between the ions do not have the motional freedom of bulk water. The relative free energy of repulsion, estimated according to Eq. 5, $\Delta\mathcal{A}^{SD}_{Na}$, is larger than the experimental estimate (on the order of $+1.7$ kcal/mol) (Becker et al., 1992). This experimental value corresponds to an effective dielectric constant of 10, which suggests that the electrostatic ion repulsion is more shielded in the real system. However, the experimental estimate of the ion repulsion is based on an analysis of ion flux data in terms

of a barrier-hopping model (see Fig. 1). It is possible that the binding free energy of the singly and doubly occupied channel states deduced from such analysis is not a true equilibrium value.

Despite the approximations involved, the calculations serve as an illustration of the various factors that must be taken into account for a meaningful study of the thermodynamics of multiple occupancy in ion channels. In particular, for detailed free energy simulations involving charged species, it is essential to account properly for finite size effects (see the above calculations). In addition, the calculations show the importance of the second order polarization energy in obtaining the correct magnitude for the free energy of cations in the channel (see the Appendix). Moreover, the calculations make clear that an approach based on the complete free energy of charging is not sufficiently accurate for a study of the influence of ion size on the thermodynamic factors involved in double ion occupancy. Generally, the calculation of small free energy differences between ions with similar radii are more accurate than the calculation of overall charging free energies. Furthermore, those free energy differences are expected to be much less sensitive to the finite size of the simulation system. In the simplest approximation, there are no finite size corrections because the charge of the ion does not change. This is the approach that was taken here to study the relative free energy between the various ions in bulk water and in the singly and doubly occupied gramicidin channel.

Relative free energies of single occupancy and in water

The free energy differences $\Delta\mathcal{A}_{ij}^{S}$ are reported in Table 6. Combining the relative free energies with the estimate of the free energy of Na^+ in bulk water and in the singly occupied channel (Table 6), we obtain estimates of the absolute free energies of the five cations. Finite size corrections were not included for the calculated relative free energies because the total charge in the simulation system remains constant. In the present approximation, atomic polarizability coefficients were assigned only to the peptide atoms and not to the water. Polarization effects could be more important for the smaller ions (Corongiu and Clementi, 1989; Dang et al., 1991), although it is possible to parameterize fixed charge models that yield correct thermodynamical and structural results (Åqvist, 1990; Jorgensen and Severance, 1993).

The agreement between the calculated free energies and the experimental chemical potential is satisfactory. For Li^+ and Na^+ in bulk water, the calculated values given in Table 6 are somewhat more negative than the experimental values whereas the interactions of these ions with a single water molecule are close to the experimental values (see Table 2). Although it would be possible to reproduce exactly the experimental free energies with small modifications of the ion nonbonded parameters (Åqvist, 1990), this approach was not taken. For example, a change of 0.5 kcal/mol in the cation-*N*-methylacetamide interaction energy can result in a change of several kcal/mol in the free energy (see also Roux and Karplus, 1991a). To a first approximation, such minor changes in the interaction energies are expected to affect equivalently the free energy differences in the singly and doubly occupied states, which is the primary concern of this paper.

Relative free energy of double occupancy

The free energy differences, $\Delta\mathcal{A}_{ij}^{S}$ and $\Delta\mathcal{A}_{ij}^{D}$ reported in Table 6 were used with Eq. 7 to estimate the relative single-to-double occupancy factor $\Delta\Delta\mathcal{A}_{ij}^{SD}$. The results are given in Table 7. The calculations show a clear tendency for the larger cations to be bound more favorably in doubly occupied channels, in agreement with experiment. To understand the origin of this behavior, the relative free energy differences, $\Delta\Delta\mathcal{A}_{ij}^{SD}$ were decomposed into various contributions by using the thermodynamic integration formula (Gao et al., 1989)

$$\Delta\Delta\mathcal{A}_{ij}^{SD} = \int_{\lambda_i}^{\lambda_j} d\lambda \left[\left\langle \frac{\partial U}{\partial \lambda} \right\rangle_{(\lambda)}^{D} - 2\left\langle \frac{\partial U}{\partial \lambda} \right\rangle_{(\lambda)}^{S} \right]. \quad (20)$$

As $\partial U/\partial\lambda = \partial u_\alpha/\partial\lambda$, where u_α represents the E_{core} and E_{vdW} interactions of type α atoms of the solvent and the channel with the ion, we have:

$$\Delta\Delta\mathcal{A}_{ij}^{SD} = \sum_{\alpha} \int_{\lambda_i}^{\lambda_j} d\lambda \left[\left\langle \frac{\partial u_\alpha}{\partial \lambda} \right\rangle_{(\lambda)}^{D} - 2\left\langle \frac{\partial u_\alpha}{\partial \lambda} \right\rangle_{(\lambda)}^{S} \right], \quad (21)$$

where λ_i and λ_j correspond to the thermodynamic integration parameter related to ions of type i and j. The decomposition is path dependent, and the present path has been chosen to demonstrate the origin of the free energy difference in the presence of the full electrostatic interactions of the charged ions. This is analogous to the Cl^- to Br^- alchemical transformation that has been considered recently to make clear the utility of the path dependence in free energy decomposition (Boresch et al., 1994). The decomposition of $\Delta\Delta\mathcal{A}_{ij}^{SD}$ into its dominant contributions is given in Table 7. It shows that the single file water inside the channel is primarily responsible for the observed trend; the carbonyl oxygens contributions are smaller and in the opposite direction. As the perturbations involve a change in the short range function $u_\alpha(r)$, the contributions from atoms that are not in direct contact with the ion are negligible. The sum of the water and carbonyl contribution does not yield the exact free energy increments because the latter were calculated with the free energy perturbation expression, Eq. 8, whereas the former were calculated with a discretized form of the thermodynamic integration formula, Eq. 21.

To gain more insight on the structural origin of the free energy contribution of the single file water molecule, the averages $\langle \partial u_\alpha/\partial\lambda \rangle_{(\lambda)}^{(S)}$ and $\langle \partial u_\alpha/\partial\lambda \rangle_{(\lambda)}^{(D)}$ in Eq. 21 are expressed in terms of distribution functions, that is,

$$\left\langle \frac{\partial u_\alpha}{\partial \lambda} \right\rangle_{(\lambda)}^{(S)} = \int dr \left(\frac{\partial u_\lambda(r;\lambda)}{\partial \lambda} \right) \rho_\alpha^S(r;\lambda), \quad (22)$$

and

$$\left\langle \frac{\partial u_\alpha}{\partial \lambda} \right\rangle_{(\lambda)}^{(D)} = \int dr \left(\frac{\partial u_\alpha(r;\lambda)}{\partial \lambda} \right) \rho_\alpha^D(r;\lambda), \quad (23)$$

where $\rho^S(r; \lambda)$ is the radial distribution function for a given value of λ as a function of the distance r between the ion and an atom of type α in the singly occupied state and $\rho^D(r; \lambda)$ is the corresponding distribution function for the doubly occupied state. The relative free energy difference is thus

$$\Delta\Delta\mathcal{A}_{ij} = \sum_\alpha \int_{\lambda_i}^{\lambda_j} d\lambda \int dr \left(\frac{\partial u_\alpha(r)}{\partial \lambda}\right)[\rho_\alpha^D(r; \lambda) - 2\rho_\alpha^S(r; \lambda)] \quad (24)$$

$$= \sum_\alpha \int_{\lambda_i}^{\lambda_j} d\lambda \int dr \left(\frac{\partial u_\alpha(r)}{\partial \lambda}\right)\Delta\rho_\alpha^{SD}(r; \lambda),$$

where $\Delta\rho_\alpha^{SD}(r; \lambda) = [\rho_\alpha^D(r; \lambda) - 2\rho_\alpha^S(r; \lambda)]$ is the difference between the distribution functions of the singly and doubly occupied state evaluated with thermodynamic integration parameter λ. The ion-ion van der Waals interaction (although its magnitude is negligible) is included implicitly in this expression.

The radial distribution function of Na^+ with the oxygen of the single file water molecules inside the channel are shown in Fig. 3*A* for the singly and doubly occupied states (the singly occupied case has been multiplied by 2 as in Eq. 24). It is observed that the maximum in the radial distribution function between the ion and the oxygen of the nearest single filed water molecule inside the channel is slightly smaller in the singly occupied channel. The difference in average radial distribution functions, $\Delta\rho_\alpha^{SD}(r; \lambda_{Na})$, shown in Fig. 3*B*, is negative at small r. Choosing the thermodynamic parameter λ to represent ions of progressively increasing size, i.e., λ_i corresponds to the smaller cation and λ_j corresponds to the larger cation, the partial derivative $\partial u_\alpha(r; \lambda)/\partial\lambda$ (evaluated for λ corresponding to Na^+), shown in Fig. 3*C*, has a very large positive value at small r. Thus, it follows that the integral in Eq. 24 gives rise to a negative relative free energy of double occupancy $\Delta\Delta\mathcal{A}_{ij}^{SD}$. As shown in Fig. 4, the function $\Delta\rho_\alpha^{SD}(r; \lambda)$ is also negative at small r for Li^+, K^+ Rb^+, and Cs^+. The size dependence arises from the fact that the ion-water core repulsion varies less abruptly in the case of larger ions, e.g., for a standard ion-water Lennard-Jones 6–12 potential with core size $\lambda\sigma$, the partial derivative involved in Eq. 24 is:

$$\frac{\partial}{\partial\lambda}(u_{LJ}(r; \lambda\sigma))\Big|_{\substack{(r=\sigma)\\(\lambda=1)}} = \frac{24\epsilon}{\sigma}. \quad (25)$$

Thus, the relative stability of the doubly occupied channel increases with the ion size, from Li^+ to Cs^+, although the effect is more important for Li^+ and Na^+.

The origin of the free energy may be described even more simply from the average distance between the ion and its nearest single file water neighbor (water numbers 3 and 8 in Fig. 2). The average distance of the ions from the oxygen of the closest single file water molecule is given in Table 9. The distance between the ions and the nearest water oxygen is slightly shorter on average in the singly occupied state than in the doubly occupied state. This observation is consistent with the results of the free energy calculations of Table 7,

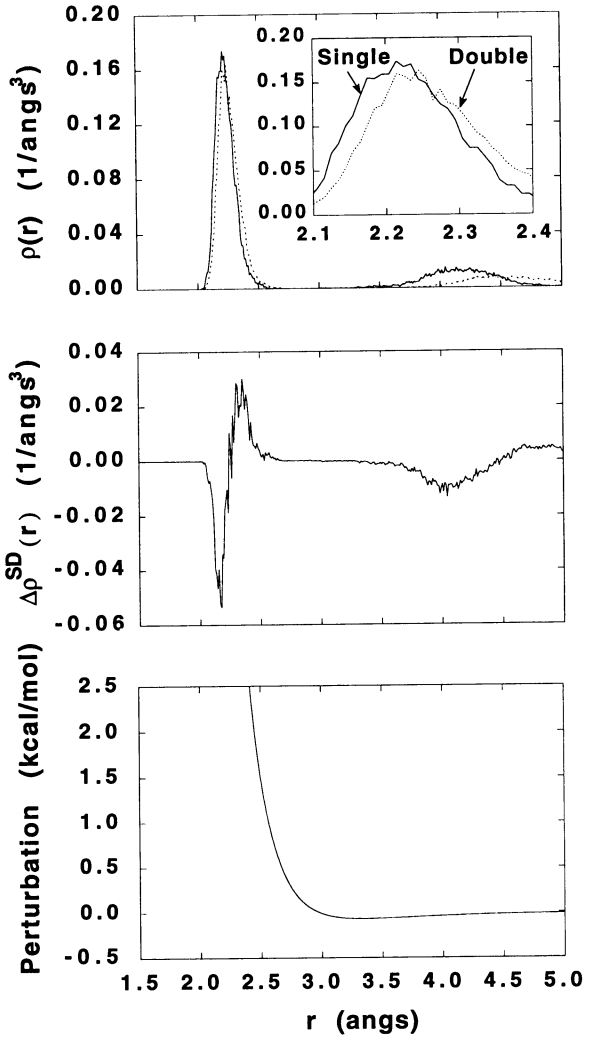

FIGURE 3 Illustration of the influence of ion size on the relative free energy of double occupancy. (*top*) Radial density distribution function $\rho^s(r)$ and $\rho^D(r)$ of Na^+ with the oxygen of the nearest internal single file water molecules (waters 3 to 8 on Fig. 2) in the singly (solid curve) and doubly (dashed curve) occupied channel states. The singly occupied case is multiplied by 2 as in Eq. 24. (*middle*) The difference between the two curves, $\Delta\rho^{SD}(r)$, is shown for Na^+. (*bottom*) The perturbation in the ion-water oxygen potential, $[u_\alpha(r;\lambda_{Na}) - u_\alpha(r;\lambda_x)]$ where X represents an intermediate cation between Na^+ and K^+. The function is large and positive at short distances because the ion size is increasing.

which indicate that the solvation of the small cations is relatively more favorable in the singly occupied channel.

The free energy difference from singly to doubly occupied state of the channel arises from a very small perturbation of the ion-water distribution function; i.e., the average distance with the nearest neighbor is increased by only 0.04 Å on average in going from the singly to the doubly occupied state (see Table 9). This small perturbation of the average ion-water distance suggests that the configuration of the water molecules inside the channel differs in the presence of one or two ions. To analyze the spatial arrangement of the water molecules, the linear density of the oxygen, $\rho(x)$, was calculated for the water-filled channel with no ion, and for the

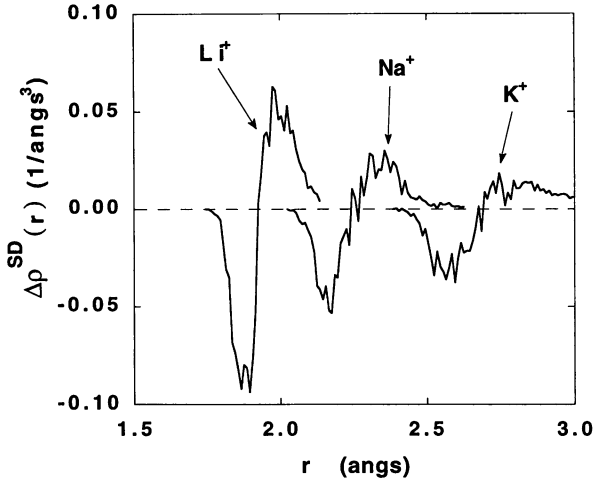

FIGURE 4 Difference in ion-water oxygen radial distribution function between the singly and doubly occupied channel states for Li^+, K^+, Rb^+, and Cs^+.

TABLE 9 Average distance with single file water (Å)*

Ions	Singly occupied	Doubly occupied
Li^+	1.92 (0.05)	1.95 (0.07)
		1.93 (0.06)
Na^+	2.24 (0.08)	2.28 (0.10)
		2.27 (0.09)
K^+	2.65 (0.10)	2.76 (0.17)
		2.68 (0.12)
Rb^+	2.86 (0.14)	2.85 (0.14)
		2.87 (0.17)
Cs^+	3.02 (0.14)	3.07 (0.15)
		3.09 (0.16)

*The rms fluctuations are given in parentheses.

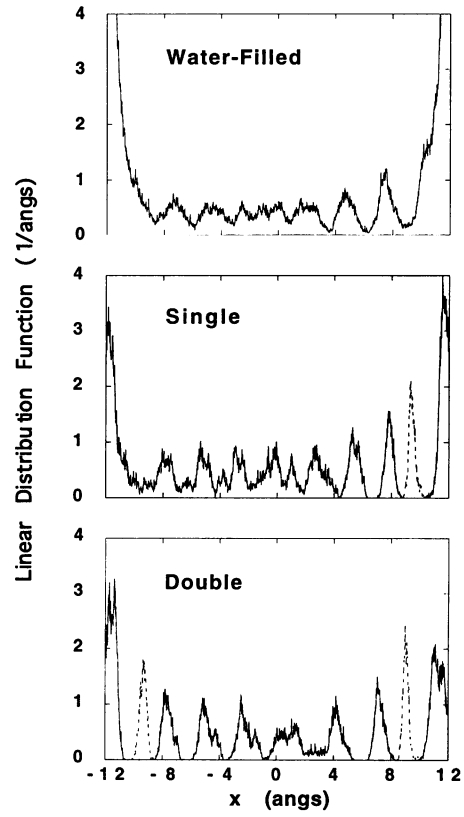

FIGURE 5 Water-oxygen linear distribution function, $\rho(x)$, along the x axis the channel. The cases of the unoccupied (water-filled channel) and single and double occupancy by Na^+ ion are shown. The distributions were not symmetrized.

singly and doubly occupied channel with Na^+. The results are shown in Fig. 5. The single file waters are sensitive to the presence or absence of ions. In the absence of ions the water molecules are distributed rather uniformly throughout the channel, with slightly higher densities for specific sites around ±5 and ±7.5 Å near the C-termini of the monomers. The small asymmetry in the average density is due to the statistical fluctuations. The potential of mean force of the water molecules along the axis of the channel can be expressed as $w(x) \sim -k_B T \ln[\rho(x)]$ (Roux and Karplus, 1991b). Thus, according to the variations in the linear density, there are no large free energy barriers opposing the movements of water molecules along the channel axis. The presence of one or two ions has a marked ordering effect on the water molecules. It is observed that the linear density has pronounced maxima for the waters in direct contact with the ions and all the other maxima are also increased. Moreover, the single file water chain is slightly displaced towards the ion in the singly occupied case; the maximal density for the Na^+ is at −9.30 Å and the nearest water peaks are at −7.79, −5.25, and −3.62 Å whereas the maximal density for the Na^+ is at −9.26 Å and the nearest water peaks are at −7.89, −5.10, and −2.48 Å in the doubly occupied case (see Fig. 5).

Because the water molecules also possess orientational degrees of freedom, the changes caused by the presence of the ions cannot be fully understood in terms of the linear distribution function of the oxygens. For example, one important aspect of the spatial arrangement of the single file waters results from the fact that their dipoles have to take a favorable orientation to interact with the ions. The close relationship between the position of the water molecules and their orientation is better described by the joint distribution function, $\rho(x, \cos\theta)$, where $\cos\theta$ is the cosine of the angle between the channel axis and the director of the single file waters, defined as the unit vector pointing from the midpoint between the two hydrogens to the oxygen. The joint distribution function $\rho(x, \cos\theta)$ in the cases of the unoccupied water-filled channel and the Na^+ singly and doubly occupied states are shown in Fig. 6. In the absence of ions the water distribution takes on a bimodal distribution in accord with the symmetry of the dimer channel. On average, the 10 water molecules located inside the channel are oriented in single file along the axis, with their oxygens pointing outward toward the bulk region. At the center of the dimer their orientation is more disordered where the symmetry is inverted. In the presence of one or two ions the distribution is modified markedly. In the singly occupied channel, all of the internal water molecules along the axis of the channel are oriented with their oxygens pointing towards the ion. The orientation of the six nearest single file waters is maintained whereas the seventh water has more freedom to reorient. In the doubly

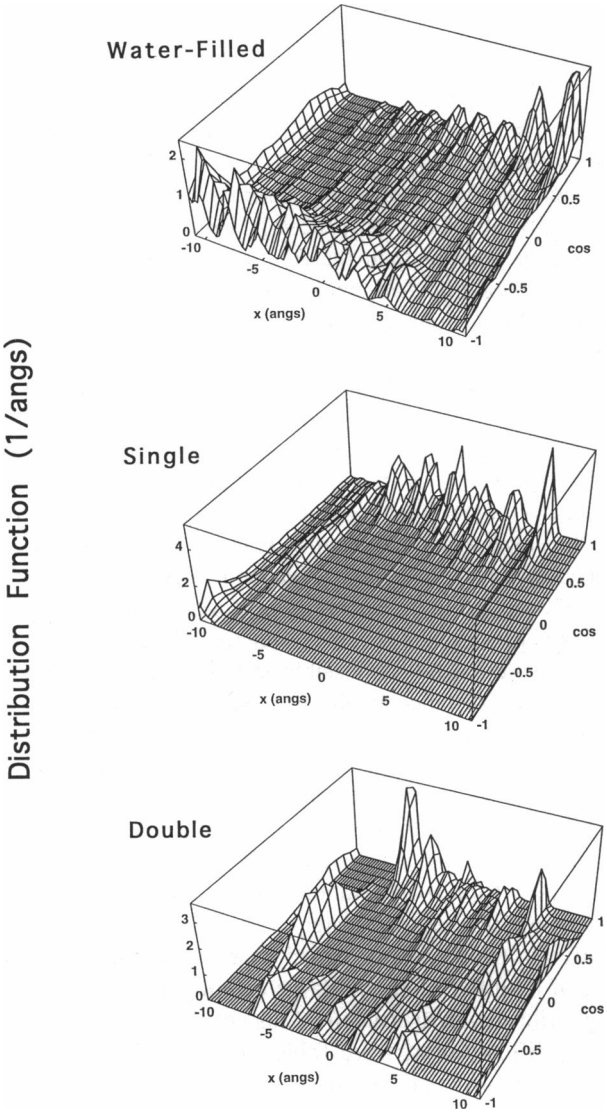

FIGURE 6 Joint distribution function of the water-oxygen position x along the channel axis and the projection of the water director onto the x axis $\rho(x, \cos)$, where $\cos = \hat{e} \cdot \hat{x}$. The director of a water molecule, $\hat{e}$, is defined as the unit vector pointing from the midpoint between the two hydrogens to the oxygen. The cases of unoccupied (water-filled channel) and single and double occupancy by Na^+ ion are shown. The distributions were not symmetrized.

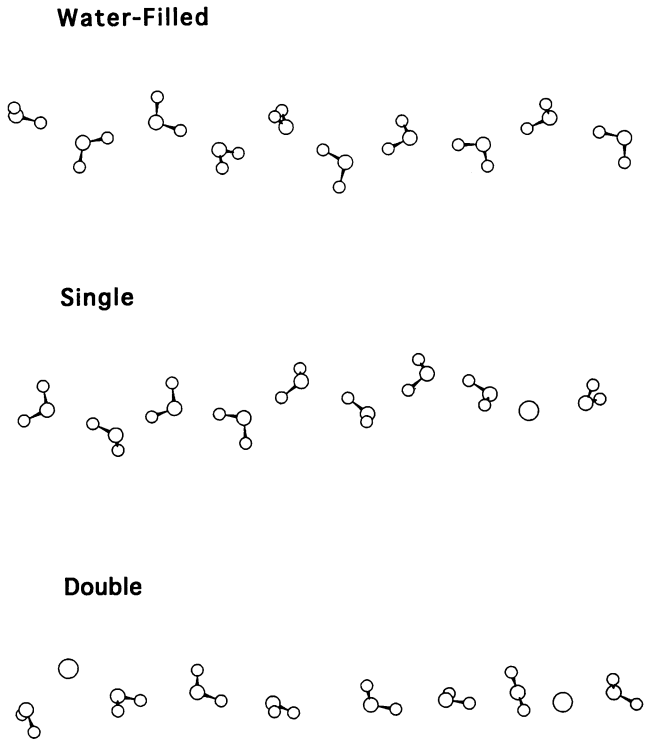

FIGURE 7 Configurations of the single file water taken from the simulation of the water-filled channel (A), and the simulation of the singly and doubly occupied channel with Na^+ (B and C).

occupied channel the picture is very different due to the frustration imposed upon the single file waters by the presence of two ions. The orientational distribution is strongly perturbed and no specific direction seems to be favored, although the nearest neighbor waters have their oxygens closer to the ion than their hydrogens. Typical configurations of the single-file waters are shown in Fig. 7 for the singly and doubly occupied states with Na^+, as well as for the water-filled channel.

To gain more insight on the solvation structure in the channel, the oxygen-oxygen and oxygen-hydrogen pair distribution functions of the six internal single file water molecules (numbers 3 to 8 in Fig. 2) were calculated for the water-filled channel and for the channel with Na^+ in the singly and doubly occupied states. The distribution functions are shown in Fig. 8. In the unoccupied channel the average oxygen-oxygen distance between nearest neighbors is approximately 2.73 Å whereas it is reduced to 2.71 Å in the singly occupied channel and increased to 2.79 Å in the doubly occupied channel. Similarly, the average water-water hydrogen bonds are affected. In the unoccupied channel the average oxygen-hydrogen distance between nearest neighbors is approximately 1.83 Å, reduced to 1.79 Å in the singly occupied channel and increased to 1.91 Å in the doubly occupied channel. These observations suggest that the response of the internal single file water molecules to the presence of ions in the binding sites may be described qualitatively in terms of an elastic spring relative to the unoccupied channel, taken as the reference relaxed state. In the singly occupied channel the water molecules are strongly attracted toward the ion, due to the long range electrostatic interactions, and the single file is slightly compressed. In the doubly occupied channel the two ions are competing for the internal water molecules and the single file is stretched. Association of the internal single file waters with the channel backbone also contributes to the response in the presence of one or two ions. The water-hydrogen carbonyl-oxygen radial distribution function, is shown in Fig. 9 for the two occupancy states of the channel. The height of the first peak in the radial distribution function is significantly reduced in the doubly occupied channel relative to the singly occupied channel. The distribution function of the water-filled channel is almost identical to that of the

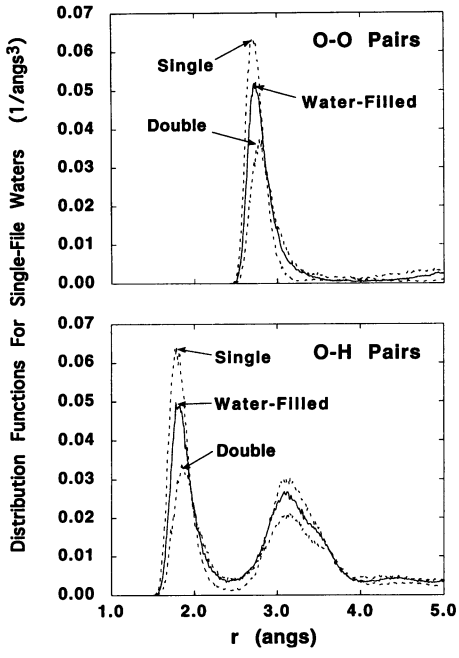

FIGURE 8 (*A*) Water-oxygen water oxygen radial distribution function for the six water molecules located inside the channel (water numbers 3 to 8 in Fig. 2). The cases of unoccupied channel and single and double occupancy by Na^+ are shown. (*B*) Water-oxygen water-hydrogen radial distribution function for the six water molecules located inside the channel. The cases of unoccupied channel and single and double occupancy by Na^+ are shown.

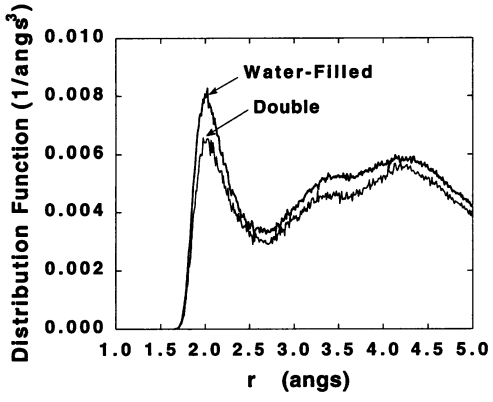

FIGURE 9 Carbonyl-oxygen water-hydrogen radial distribution function for the six water molecules located inside the channel (water numbers 3 to 8 in Fig. 2). The cases of unoccupied channel and double occupancy by Na^+ are shown. For the sake of clarity, the radial distribution function is not shown for the singly occupied channel because it is superimposed on that of the unoccupied channel.

singly occupied channel and is not shown. This indicates that water-carbonyl hydrogen bonding interactions are reduced in the doubly occupied channel relative to the singly occupied channel.

The peculiar structural properties of single file solvation may be responsible for the response to the presence of a second ion in the channel. It is suggestive to compare the solvation structure of the ions in the single file with that in bulk solution. The radial distribution function of the ion-water oxygen, calculated in bulk solvent (with the spherical system of 250 waters), is shown in Fig. 10. Comparison of R_{max}, the position of the first peak in the radial distribution function in single file and in bulk solution, given in Table 10, shows that the single filing of the water imposed by the gramicidin channel leads to a closer contact with the nearest water. For all of the ions, the R_{max} for the singly occupied channel is smaller than the R_{max} for the doubly occupied channel, which is itself smaller or equal to the R_{max} in bulk solution. In the doubly occupied channel, the ion-water contact with the nearest single file water is perturbed relative to the singly occupied channel; e.g., for Li^+ the distance with the nearest water molecule is 1.90 Å in the singly occupied channel, whereas it is 1.93 Å in the doubly occupied channel and in bulk water (the position of the maximum is consistent with the average distances given in Table 9). In fact, the R_{max} for the singly occupied channel is close to the optimal distance for an isolated water molecule in vacuum (e.g., 1.88 Å for Li^+, see Table 2). Such a close contact with water molecules is prevented by water-water repulsion around an ion in bulk solution but is possible in single file solvation. In general, the distance to the nearest waters located in the mouth of the channel (in the direction of the bulk water) is slightly larger than in the channel direction; e.g., the average distance of the ion with the oxygen of the closest water molecule (water numbers 1 and 10 in Fig. 2) are 2.31 and 2.34 Å for Na^+; the latter is similar to that observed in bulk solution (see Table 10). Although the tendency toward closer contact with the nearest water in a singly occupied channel relative to the doubly occupied channel is observed in the case of both the small and large cations, the change in the single file solvation structure does not result in similar free energy difference, A_{ij}^{SD} (see Table 7). The single file of water is relatively ordered and makes a tight contact with the ion in the singly occupied channel; it is less ordered and makes a looser contact with the ions in the doubly occupied channel. It follows from the average hydration structure in the pore

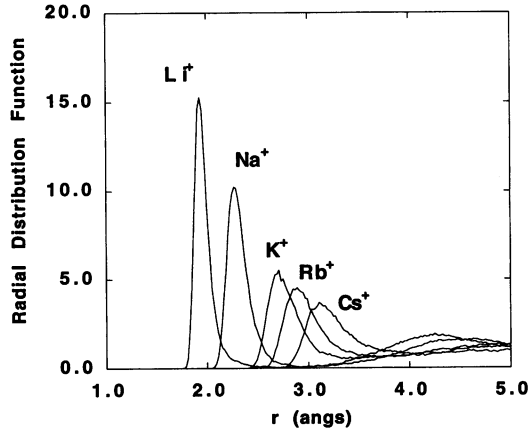

FIGURE 10 Na^+-water-oxygen radial density distribution function in bulk water calculated in a sphere of 120 TIP3 molecules. The distribution function was normalized by the bulk solvent density.

TABLE 10 Ion-Water radial distribution function, R_{max} (Å)*

Ions	Bulk water‡	Singly occupied gramicidin A	Doubly occupied gramicidin A
Li^+	1.93 (4.3)	1.90	1.93
Na^+	2.27 (5.8)	2.22	2.25
K^+	2.71 (7.0)	2.60	2.62
Rb^+	2.89 (8.5)	2.77	2.77
Cs^+	3.11 (10.5)	2.99	3.00

*R_{max} is defined as the position of the maximum in the cation-water oxygen radial distribution function.

‡ The hydration numbers, given in parentheses, are the average number of water molecules in the first shell defined from the position of the minimum in the radial distribution function.

that the reversible work needed to increase the radius of an ion is slightly larger in the singly occupied channel than in the doubly occupied channel. This observation may be related to a simplified description of ion solvation. In an analysis of the molecular basis of the Born model of solvation, it was shown that the first peak in the ion-water radial distribution function can be interpreted as the classical ionic radius of hydration that determines the dominant contribution to the solvation free energy of a charged solute (Roux et al., 1990). In the present case, a simple way to express the observed trend might be to say that the effective ionic size in a single file is affected by the channel occupancy. As the ionic radius is slightly smaller in a singly occupied channel relative to a doubly occupied channel and bulk water, this is expected to lead to a small, channel occupancy-dependent variation of the relative binding free energies of cations. Consequently, the singly occupied state is more favorable for the smaller ions. However, the trend is a relative effect that is independent of the absolute free energy of ions in the channel binding site (see Table 6). Thus, an equivalent statement would be that the doubly occupied state is less unfavorable in the case of the larger ions.

CONCLUDING DISCUSSION

The structural and thermodynamic factors responsible for the properties of the single and double occupancy states of the gramicidin channel were investigated with molecular dynamics simulations and free energy perturbation methods. An ion-peptide potential function including first and second order polarization was developed for the five common cations. The parameters for Li^+, Na^+, and K^+ were primarily based on calculated ab initio energy surfaces with the *N*-methylacetamide molecule (Roux and Karplus, 1995); the parameters of the larger cations Rb^+ and Cs^+ were obtained empirically on the basis of experimental solvation data in bulk water and on ionic radii.

The parameterization of the microscopic model was validated by calculating the absolute free energy of Na^+ in bulk water and in the channel. The charging free energy of Na^+ was estimated in a bulk water sphere and in the singly and doubly occupied gramicidin channel; the free energy of the other ions was deduced from the result obtained for Na^+ by using the calculated free energy differences. For all the cations the free energies calculated in a bulk water sphere are close in magnitude to the corresponding experimental value of the chemical potential in bulk water; for the smaller ions (Li^+ and Na^+) the calculation overestimates the solvation free energy. Nonadditive second order polarization energy, in addition to the first order energy, is necessary to obtain the correct magnitude for the free energy of Na^+ in the channel; its contribution amounts to almost 40% of the total free energy (see Appendix) (Roux, 1993). The contribution of corrections for the finite size of the system to the free energy of charging is significant and must be included for meaningful results. In the present study a correction based on continuum electrostatics derived from a multiple expansion for a spherical cavity was used although other approaches, such as the numerical solution of the Poisson-Boltzmann on a discrete grid (Gilson and Honig, 1988), are also possible.

The relative single-to-double occupancy free energy was calculated for the five ions. The calculations reveal, in agreement with experimental observations (O.S. Andersen, personal communication, 1994), that the doubly occupied state is relatively more favorable for the larger ions. The origin of the trend observed in the calculations is found by thermodynamic decomposition to be due to the loss of favorable interactions between an ion and the water molecules arranged in single file inside the channel. Analysis of the radial distribution function between the ion and the oxygen of the nearest single file water molecule inside the channel shows that the maximum is systematically closer to the ion in the singly occupied channel. This observation is supported by the comparison of the average ion-oxygen distances, given in Table 9, and the position of the maximum in the radial distribution functions, given in Table 10. Small ions are better solvated in the singly occupied state than in the doubly occupied state by the single file waters; bigger ions are almost as well solvated in both occupation states. Analysis of the distribution functions related to hydrogen bonding indicates that water-water and water-channel interactions play an important role in the double occupancy response. In the singly occupied channel, the linear chain of single file waters is well ordered and the water-water hydrogen bonds between nearest neighbors are shortened relative to the water-filled channel. In the doubly occupied channel, the linear chain of single file waters is more disordered and the water-water hydrogen bonds between nearest neighbors are longer.

The number of single file waters separating the two ions in the doubly occupied channel was set to six, independent of ion type. This choice was based on the available space between the two binding sites located at each end of the channel (see above). No experimental data about the number of single file waters in the singly and doubly occupied channel are available. The present calculations demonstrate that the stability of long narrow single file pores, such as the gramicidin channel, is sensitive to the ion type involved in multiple occupancy. This is a significant result as the two ions are separated by approximately 18 Å in the doubly occupied channel.

In the doubly occupied channel, two cations are closely associated with eight water molecules (see Fig. 2). The single file corresponds to a one-dimensional ionic solution with a molarity of almost 10 M (assuming that the volume of the pore is given by a length of 25 Å and a cross section of 12.5 $Å^2$ corresponding to a radius of 2 Å). A comparison of the ion size dependence of double occupancy with the thermodynamic properties of concentrated ionic solutions is suggestive. The activity coefficient of cations in solution have a complex dependence on the ionic concentration. At very low concentrations, the activity coefficients decrease as the concentration is raised due to the long range favorable electrostatic interactions with the ionic atmosphere (this is the Debye-Hückel limiting law) (McQuarrie, 1976); at higher concentration, the activity coefficients start to increase due to unfavorable energetic factors (this is related to the salting-out effects that ions exert by raising the activity coefficients of the other solutes present in the solution, (see Ch. 7 of Hille, 1984, and the monograph by Stokes, 1979). Interestingly, a well known property of concentrated solutions of strong electrolytes is the existence of an inverse relation between the activity coefficient and the size of the cation (Robinson and Stokes, 1965); e.g., at 25°C for a 2 M solution of the salt with Cl^-, the molal activities of Li^+, Na^+, K^+, Rb^+, and Cs^+ are 0.921, 0.668, 0.658, 0.546, and 0.496, respectively. The variation of the activity coefficients in concentrated solutions has been traditionally attributed to a modification of the ion-solvent interactions due to the presence of the other nearby ions (Conway, 1979). Such interpretation is supported by computer simulations. It was observed in molecular dynamics of NaCl aqueous solutions that the intensity of the first and second maxima in the ion-solvent radial pair correlation function are lower at higher salt concentrations; which corresponds to a less definite first and second hydration shell in the more concentrated solution (Heinzinger, 1985). The decrease in cation-solvent association in concentrated solution has been also observed in neutron scattering experiments (Enderby, 1983). In the present study, the microscopic factors favoring double occupancy by larger ions were related to the change in the pair correlation function of the ion relative to the single file waters. Thus, it may be that the mechanism favoring the double occupancy of larger over smaller cations in the gramicidin channel can be related to a more general property of cation solvation by water.

On a speculative note, the thermodynamic trend found here could be an explanation for the existence of a large number of biological K channels that function on the basis of multiple occupancy (Hille and Schwarz, 1978; Hodgkin and Keynes, 1955; Pallota and Wagoner, 1992), whereas most of the data about Na channels can be explained by a single ion model (Begenisich, 1987; French et al., 1994; Hille, 1975; Naranjo and Latorre, 1993). As mentioned in the Introduction, it has been suggested that the influence of ion-ion interactions in multiply occupied single file is an essential component of the mechanisms by which the K channels succeed in achieving high selectivity while maintaining a large ionic conductance (Neyton and Miller, 1988a; Neyton and Miller, 1988b). It may not be as easy for nature to make a similar highly selective single file Na channel functioning on the basis of multiple occupancy. Based on the present free energy calculations, double occupancy by K^+ in a single file pore is not thermodynamically very unfavorable relative to single occupancy. This factor may have contributed to the evolution of the biological K channels that are very selective and highly conductive single file pores functioning on the basis of multiple ion occupancy. Although biological Na channels are thought to derive from Ca channels (Hille, 1984), they may have evolved to function predominantly as single ion pores, because a larger free energy cost is attached to multiple occupancy by the smaller ions in single file solvation. It is interesting to note that double occupancy of the Na channel is much more evident with NH_4^+ as the permeant ion (Begenisich and Cahalan, 1980; Begenisich, 1987) as it is a cation with an ionic radius (1.4 Å) closer to that of K^+ (1.33 Å) (Hille, 1984).

The discrete nature of the water molecules in the single file channel is another factor that may play a role in the relative likelihood of single versus double occupancy. In the gramicidin channel the distance between the two binding sites is nearly commensurate with the diameter of the water molecules; i.e., the binding sites are separated by approximately 18 Å and there is room for six water molecules after subtracting the diameter of the cations. It is possible that the observed trend in single and double occupancy can be affected by chemical modifications of the gramicidin channel. The simulations show that the factors controlling double occupancy in the gramicidin channel result from the single file solvation and are a function of its structure. This suggests the use of chemically modified gramicidin channels of different lengths to gain more insight into the thermodynamics of single and double ion occupancy. For example, by addition or deletion of one (L,D) unit near the NH_2 terminus of the gramicidin monomer, it is possible to synthesize slightly longer or shorter dimer channels without causing large conformational changes at the binding sites. Because one (L,D) unit corresponds to a length of 1.55 Å (Roux and Karplus, 1991a), the distance between the binding sites could be varied from −3.10 Å (one deletion per monomer in homodimers) to ±1.55 Å (one deletion or insertion in hybrid dimers) and +3.10 (one insertion per monomer in homodimers). As the diameter of one water molecule is approximately 2.8 Å, such modifications would influence the properties of the water molecules inside the channel and could, thereby, modulate the relative thermodynamics of single and double ion occupancy.

APPENDIX

Importance of polarization energy

To illustrate the importance of the second order polarization energy $E_{pol}^{(2)}$, the free energy of charging of Na^+ in the channel was also calculated by including only the first order polarization $E_{pol}^{(1)}$ (see Eqs. 13 and 14). With a slow growth procedure, a forward trajectory of 50 ps, in which the charge was varied from 0 to 1, yielded a free energy of −142 kcal/mol, and a

backward trajectory of 50 ps, in which the charge varied from 1 to 0, yielded a free energy of +136 kcal/mol, for an average of −139 kcal/mol. This result contrasts sharply with the value of −100 kcal/mol obtained by including both the first and second order polarization (see Table 5). The large difference implies that the free energy contribution of second order polarization, $\mathcal{A}^{(2)}_{pol}$, corresponds to approximately +39 kcal/mol. It can be shown that this result is consistent with an estimate obtained by the free energy perturbation method. The contribution of second order polarization energy was calculated in a single perturbation step with Eq. 8 from two trajectories of 15 ps. The first trajectory was generated with only first order polarization, and the second trajectory was generated with both first and second order polarization (the results of the two one-step perturbations are combined together for better convergence). This yields:

$$\mathcal{A}^{(2)}_{pol} = \tfrac{1}{2}[-k_B T \ln\langle e^{-E^{(2)}_{pol}/k_B T}\rangle_{(1)} + k_B T \ln\langle e^{+E^{(2)}_{pol}/k_B T}\rangle_{(2)}]. \quad (26)$$

The result is +45 kcal/mol for Na^+. These calculations show the importance of the second order polarization energy in obtaining the correct value for the free energy of Na^+ in the channel.

B. Roux is supported by grants from the Medical Research Council of Canada and from the Fonds pour la Recherche en Sante du Quebec. This work was supported by a grant from the U.S. National Science Foundation (M. Karplus).

REFERENCES

Åqvist, J. 1990. Ion water interaction potential derived from free energy perturbation simulations. *J. Phys. Chem.* 94:8021–8024.

Åqvist, J., and A. Warshel. 1989. Energetics of ion permeation through membrane channels. *Biophys. J.* 56:171–182.

Arseniev, A. S., I. L. Barsukov, and V. F. Bystrov. 1986. Conformation of gramicidin A in solution and micelles: two dimensional ^{1}H NMR study. *In* Chemistry of Peptides and Proteins, Vol. 3. Y. A. Ovchinnikov, W. Voelter, E. Bayer, and V. T. Ivanov, editors. W. Voelter Co., Berlin. 127–158.

Arseniev, A. S., V. F. Bystrov, T. V. Ivanov, and Y. A. Ovchinnikov. 1985. ^{1}H-NMR study of gramicidin-A transmembrane ion channel: head-to-head right-handed, single stranded helices. *FEBS Lett.* 186:168–174.

Becker, M. D., R. E. Koeppe II, and O. S. Andersen. 1992. Amino acid substitutions and ion channel function: model-dependent conclusions. *Biophys. J.* 62:25–27.

Begenisich, T. 1987. Molecular properties of ion permeation through sodium channels. *Annu. Rev. Biophys. Chem.* 16:247–263.

Begenisich, T., and M. Cahalan. 1980. Sodium channel permeation in squid axons: reversal potential experiments. *J. Physiol.* 307:217–242.

Berendsen, H. C., J. P. Postma, and J. R. Haak. 1982. The thermodynamics of cavity formation in water, a molecular dynamics study. *Farad. Symp. Chem. Soc.* 17:55–67.

Boresch, S., G. Archontis, and M. Karplus. 1994. Free energy simulations: the meaning of the individual contributions from a component analysis of proteins. *Proteins.* 20:25–33.

Born, M. 1920. Volumen und hydratationswarme der ionen. *Z. Phys.* 1:45.

Brooks, B. R., R. E. Bruccoleri, B. D. Olafson, D. J. States, S. Swaminathan, and M. Karplus. 1983. CHARMM: a program for macromolecular energy minimization and dynamics calculations. *J. Comput. Chem.* 4:187–217.

Brooks, C. L. III, and M. Karplus. 1983. Deformable stochastic boundaries in molecular dynamics. *J. Chem. Phys.* 79:6312–6325.

Brooks, C. L. III, M. Karplus, and B. M. Pettitt. 1988. Proteins: a theoretical perspective of dynamics, structure and thermodynamics. *In* Advances in Chemical Physics, Vol. LXXI. I. Prigogine and S. A. Rice, editors. John Wiley & Sons, New York.

Brunger, A., C. L. Brooks III, and M. Karplus. 1984. Stochastic boundary conditions for molecular dynamics simulations of ST2 water. *Chem. Phys. Lett.* 105:495–500.

Chiu, S. W., E. Jakobsson, S. Subramaniam, and J. A. McCammon. 1991. Time-correlation analysis of simulated water motion in flexible and rigid gramicidin channels. *Biophys. J.* 60:273–285.

Clementi, E., H. Kistenmacher, W. Kolos, and S. Romano. 1980. Non-additivity in water-ion-water interactions. *Theo. Chim. Act.* 55:257–266.

Conway, B. E. 1979. Activity coefficients and hydration of ions. *In* Activity Coefficients in Electrolyte Solutions. R. M. Pytkowicz, editor. CRC Press, Boca Raton, FL. 95–138.

Cornell, B. A., F. Separovic, A. J. Baldassi, and R. Smith. 1988. Conformation and orientation of gramicidin A in oriented phospholipid bilayers measured by solid state carbon-13 NMR. *Biophys. J.* 53:67–76.

Corongiu, G., and E. Clementi. 1989. Hydration free energy for Li^+ at infinite dilution with a three-body ab initio potential. *J. Chem. Phys.* 90:4629–4630.

Dang, L. X., J. E. Rice, J. Caldwell, and P. A. Kollman. 1991. Ion solvation in polarizable water: molecular dynamics simulations. *J. Am. Chem. Soc.* 113:2481–2486.

Džidić, I., and P. Kebarle. 1970. Hydration of the alkali ions in the gas phase. Enthalpies and entropies of reactions $M^+(H_2O)_{m-1} + H_2O = M^+(H_2O)_m$. *J. Phys. Chem.* 74:1466–1474.

Enderby, J. E. 1983. Neutron scattering from ionic solutions. *Annu. Rev. Phys. Chem.* 34:155.

Finkelstein, A., and O. S. Andersen. 1981. The gramicidin A channel: A review of its permeability characteristics with special reference to the single-file aspect of transport. *J. Membr. Biol.* 59:155–171.

French, R. J., J. F. Worley, W. F. Wonderlin, A. S. Kularatna, and B. K. Krueger. 1994. Ion permeation, divalent ion block and chemical modification of single sodium channels: description by single and double occupancy rate-theory models. *J. Gen. Physiol.* 103:447–470.

Friedman, H. L., and C. V. Krishnan. 1973. *In* Water: A Comprehensive Treatise, Vol. 3. F. Franks, editor. Plenum Press, New York.

Gao, J., K. Kuczera, B. Tidor, and M. Karplus. 1989. Hidden thermodynamics of mutant proteins: a molecular dynamics study. *Science.* 244: 1069–1072.

Gilson, M. K., and B. Honig. 1988. Calculation of the total electrostatic energy of a macromolecular system. *Proteins.* 4:7–18.

Goodfellow, J. M. 1982. Cooperative effects in water-biomolecule crystal systems. *Proc. Natl. Acad. Sci. USA.* 79:4977.

Goodfellow, J. M., J. L. Finney, and P. Barnes. 1982. Monte Carlo computer simulation of water-amino acid interactions. *Proc. R. Soc. Lond.* 214: 213–228.

Gourary, B. S., and F. J. Adrian. 1960. Wave functions for electron-excess color centers in alkali halide crystals. *Solid State Phys.* 10:127–247.

Heinzinger, K. 1985. Computer simulations of aqueous electrolyte solutions. *Physica.* 131B:196–216.

Hess, P., and R. Tsien. 1984. Mechanism of ion permeation through calcium channels. *Nature.* 309:453–456.

Hille, B. 1975. Ionic selectivity, saturation, and block in sodium channels: a four-barrier model. *J. Gen. Physiol.* 66:535–560.

Hille, B. Ionic Channels of Excitable Membranes. Sinauer, Sunderland, MA.

Hille, B., and W. Schwarz. 1978. Potassium channels as multi-ion single-file pores. *J. Gen. Physiol.* 72:409–442.

Hinton, J. F., J. Q. Fernandez, D. C. Shungu, W. L. Whaley, R. E. Koeppe II, and F. S. Millett. 1988. TI-205 nuclear magnetic resonance determination of the thermodynamic parameters for the binding of monovalent cations to gramicidin A and C. *Biophys. J.* 54:527–533.

Hinton, J. F., W. L. Whaley, D. C. Shungu, R. E. Koeppe II, and F. S. Millett. 1986. Equilibrium binding constant for the group I metal cations with gramicidin-A determined by competition studies and Tl^+-205 nuclear magnetic resonance spectroscopy. *Biophys. J.* 50: 539–544.

Hladky, S. B., and D. A. Haydon. 1972. Ion transfer across lipid membranes in the presence of gramicidin A. *Biochim. Biophys. Acta.* 274:294–312.

Hladky, S. B., and D. A. Haydon. 1984. Ion movements in gramicidin channels. *Curr. Top. Membr. Transp.* 21:327–372.

Hodgkin, A. L., and R. D. Keynes. 1955. The potassium permeability of a giant nerve fibre. *J. Phys.* 128:61–88.

Jorgensen, W. L., J. F. Blake, and J. K. Bucker. 1989. Free energy of TIP4P water and the free energies of hydration of CH_4 and Cl^- from statistical perturbation theory. *Chem. Phys.* 129:193–200.

Jorgensen, W. L., R. W. Impey, J. Chandrasekhar, J. D. Madura, and M. L. Klein. 1983. Comparison of simple potential functions for simulating liquid water. *J. Chem. Phys.* 79:926–935.

Jorgensen, W. L., and D. L. Severance. 1993. Limited effects of polarization for $Cl^-(H_2O)_n$ and $Na^+(H_2O)_n$ clusters. *J. Chem. Phys.* 99:4233–4235.

Ketchem, R. R., W. Hu, and T. A. Cross. 1993. High resolution conformation of gramicidin A in lipid bilayer by solid-state NMR. *Science.* 261:1457–1460.

Kirkwood, J. G. 1934. Theory of solution of molecules containing widely separated charges with application to zwiterions. *J. Chem. Phys.* 2:351.

Kirkwood, J. G. 1935. Statistical mechanics of fluid mixtures. *J. Chem. Phys.* 3:300.

Koeppe, R. E. II, J. H. Berg, K. O. Hogdson, and L. Stryer. 1979. Gramicidin A crystals contain two cation binding sites per channel. *Nature.* 279: 723–725.

Levitt, D. G. 1987. Exact continuum solution for a channel that can be occupied by two ions. *Biophys. J.* 52:455–466.

Lybrand, T. P., and P. A. Kollman. 1985. Water-water and water-ion potential functions including terms for many body effects. *J. Phys. Chem.* 83:2923–2933.

McQuarrie, D. A. 1976. Statistical Mechanics. Harper and Row, New York.

Naranjo, D., and R. Latorre. 1993. Ion conduction in substates of the batrachotoxin-modified Na^+ from toad skeletal muscle. *Biophys. J.* 64: 1038–1050.

Neyton, J., and C. Miller. 1988a. Potassium blocks barium permeation through a calcium-activated potassium channel. *J. Gen. Physiol.* 92: 549–567.

Neyton, J., and C. Miller. 1988b. Discrete Ba^{2+} block as a probe of ion occupancy and pore structure in the high-conductance Ca^{2+}-activated K^+ channel. *J. Gen. Physiol.* 92:569–586.

Olah, G. A., H. W. Huang, W. Liu, and Y. Wu. 1991. The thallium ion distribution in the gramicidin channel by X-ray diffraction. *J. Mol. Biol.* 218:847.

Pallota, B. S., and P. K. Wagoner. 1992. Voltage-dependent potassium channels since Hodgkin and Huxley. *Physiol. Rev.* 72:S49–S67.

Pauling, L. 1960. Nature of the Chemical Bond and Structure of Molecules and Crystals, 3rd ed. Cornell University Press, Ithaca, NY.

Pettitt, B. M., and P. J. Rossky. 1986. Alkali halides in water: ion-solvent and ion-ion potential of mean force at infinite dilution. *J. Chem. Phys.* 84:5836–5844.

Procopio, J., and O. S. Andersen. 1979. *Biophys. J.* 25:8a.

Reiher, W. E. III. 1985. Theoretical studies of hydrogen bonding. Ph.D. thesis. Harvard University, Cambridge, MA.

Robinson, R. A., and R. H. Stokes. 1965. Electrolyte Solutions. Butterworths, London.

Roux, B. 1993. Nonadditivity in cation-peptide interactions: a molecular dynamics and ab initio study of Na^+ in the gramicidin channel. *Chem. Phys. Lett.* 212:231–240.

Roux, B. 1995. Theory of transport in ion channels: from molecular dynamics simulations to experiments. *In* Computer Simulation in Molecular Biology. J. Goodfellow, editor. VCH, Weinheim.

Roux, B., and M. Karplus. 1994. Molecular dynamics simulations of the gramicidin channel. *Annu. Rev. Biomol. Struct. Dynam.* 23:731–761.

Roux, B., and M. Karplus. 1995. Potential energy function for cations-peptides interactions: an ab initio study. *J. Comp. Chem.* In press.

Roux, B., and M. Karplus. 1991a. Ion transport in a gramicidin-like channel: structure and thermodynamics. *Biophys. J.* 59:961–981.

Roux, B., and M. Karplus. 1991b. Ion transport in a gramicidin-like channel: dynamics and mobility. *J. Phys. Chem.* 95:4856–4868.

Roux, B., and M. Karplus. 1993. Ion transport in the gramicidin channel: free energy of the solvated right-handed dimer in a model membrane. *J. Am. Chem. Soc.* 115:3250–3262.

Roux, B., H. A. Yu, and M. Karplus. 1990. Molecular basis for the born model of ion solvation. *J. Phys. Chem.* 94:4683–4688.

Ryckaert, J. P., G. Ciccotti, and H. J. C. Berendsen. 1977. Numerical integration of the Cartesian equation of motions of a system with constraints: molecular dynamics of *N*-alkanes. *J. Comp. Chem.* 23: 327–341.

Sandblom, J., G. Eisenman, and J. Hagglund. 1983. Multioccupancy models for single-filing ionic channels: theoretical behavior of a four-site channel with three barriers separating the sites. *J. Membr. Biol.* 71:61–78.

Schagina, L. V., A. E. Grinflet, and A. A. Lev. 1978. Interaction of cation fluxes in gramicidin A channels in lipid bilayer membranes. *Nature.* 273: 243–245.

Schagina, L. V., A. E. Grinflet, and A. A. Lev. 1983. Concentration dependence of bidirectional flux ratio as a characteristic of transmembrane ion transporting mechanism. *J. Membr. Biol.* 73:203–216.

Shimada, J., H. Kaneko, and T. Takada. 1994. Performance of fast multipole methods for calculating electrostatic interactions in biomacromolecular simulations. *J. Comp. Chem.* 15:28–43.

Singh, U. C., F. K. Brown, P. A. Bash, and P. A. Kollman. 1987. An approach to the application of free energy perturbation methods using molecular dynamics. *J. Am. Chem. Soc.* 109:1607–1614.

Smith, R., D. E. Thomas, A. R. Atkins, F. Separovic, and B. A. Cornell. 1990. Solid-state ^{13}C-NMR studies of the effects of sodium ions on the gramicidin A ion channel. *Biochim. Biophys. Acta.* 1026:161–166.

Smith, R., D. E. Thomas, F. Separovic, A. R. Atkins, and B. A. Cornell. 1989. Determination of the structure of a membrane-incorporated ion channel. *Biophys. J.* 56:307–314.

Stokes, R. H. 1979. Thermodynamics of solutions. *In* Activity Coefficients in Electrolyte Solutions. R. M. Pytkowicz, editor. CRC Press, Boca Raton, FL. 1–28.

Stote, R. H., D. J. States, and M. Karplus. 1991. On the treatment of electrostatic interactions in biomolecular simulation. *J. Chim. Phys.* 88:2419–2433.

Straatsma, T. P., and H. J. C. Berendsen. 1988. Free energy of ionic hydration: analysis of a thermodynamic integration technique to evaluate free energy differences by molecular dynamics simulations. *J. Chem. Phys.* 89:5876–5886.

Straatsma, T. P., and J. A. McCammon. 1990. Molecular dynamics simulations with interaction potentials including polarization: development of a noniterative method and application to water. *Mol. Sim.* 5:181–192.

Urban, B. W., S. B. Hladky, and D. A. Haydon. 1980. Ion movements in gramicidin pores. *Biochem. Biophys. Acta.* 602:331–354.

Urry, D. W., K. U. Prasad, and T. L. Trapane. 1982a. Location of monovalent cation binding sites in the gramicidin channel. *Proc. Natl. Acad. Sci. USA.* 79:390–394.

Urry, D. W., J. T. Walker, and T. L. Trapane. 1982b. Ion interactions in (L-^{13}C) D-Val^8 and D-Leu^{14} analogues of gramicidin A: the helix sense of the channel and location of ion binding sites. *J. Membr. Biol.* 69:225–231.

Van Belle, D., I. Couplet, M. Prevost, and S. J. Wodak. 1987. Calculations of electrostatic properties in proteins. *J. Mol. Biol.* 198:721–735.

Woolf, T. B., and B. Roux. 1993. Molecular dynamics of proteins in lipid membranes: the first steps. *Biophys. J.* 64:A354.

Woolf, T. B., and B. Roux. 1994. Molecular dynamics simulation of the gramicidin channel in a phospholipid bilayer. *Proc. Natl. Acad. Sci. USA.* 91:11631–11635.

Zwanzig, R. W. 1954. High temperature equation of state by a perturbation method. *J. Chem. Phys.* 22:1420–1426.